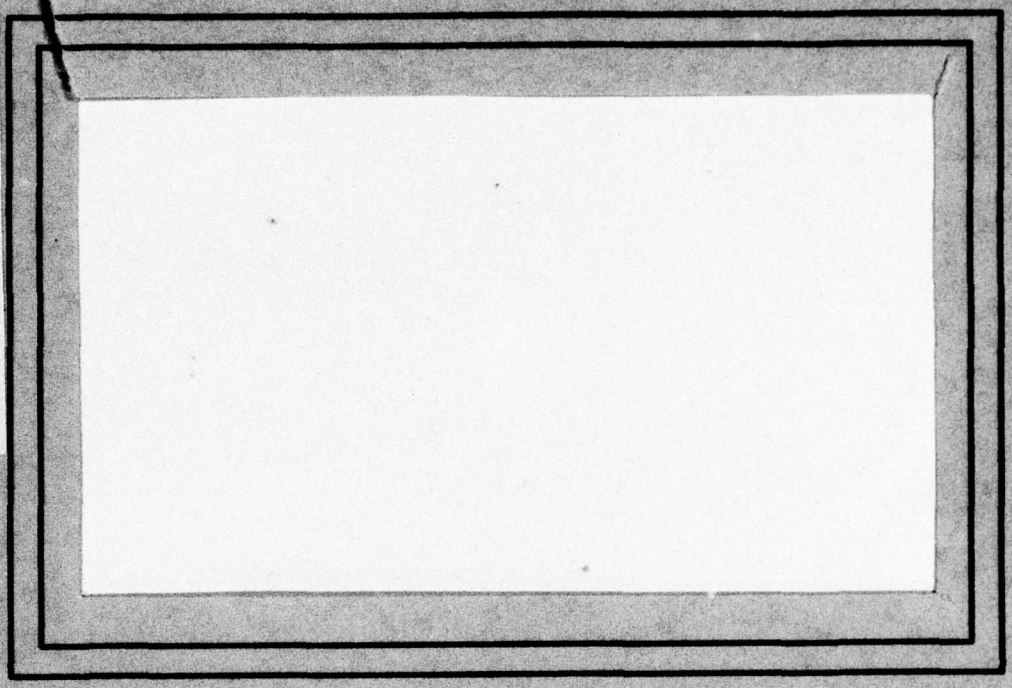

COMPUTER SCIENCE TECHNICAL REPORT SERIES

UNIVERSITY OF MARYLAND
COLLEGE PARK, MARYLAND
20742

(1)

(9) Technical rept.,

(14) TR-558
DAAG53-76C-0138

(11) July 1977

(12) 61 p.

(6) STATISTICAL ANALYSIS OF SOME EDGE OPERATORS.

(10) Durga P./Panda
Computer Science Center
University of Maryland
College Park, MD 20742

ABSTRACT

A statistical analysis of the responses of some linear and nonlinear edge operators is presented. The input image is treated as a stationary random field from a context independent ensemble. Several stochastic properties of the output images are predicted. Some experimental results are given.

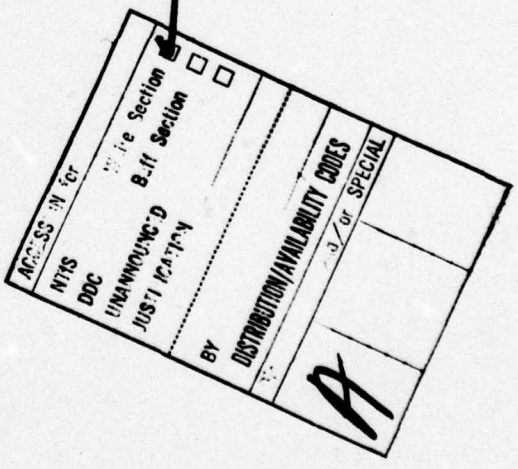

(15) The support of the U. S. Army Night Vision Laboratory under Contract DAAG53-76C-0138, ARPA Order-3206 is gratefully acknolwedged, as is the help of Mrs. Shelly Rowe in preparing this paper.

1473

403 018

1. Introduction

Often statistical analysis of the response of an image operator is necessary in order to determine in some optimal way the nature of further processing of the response. For example, edge detection is usually done by thresholding the output of an edge-sensitive operator; the false alarm and false dismissal rates of this process depend on the statistics of the edge operator responses. As another example, thinning of edges by local nonmaximum suppression [1] may be done in an optimal way if the average neighborhood size containing a local maximum is known. Thus neighborhood size can be derived from the average spatial density of local maxima of the edge responses for the given input picture.

In this paper we discuss statistical properties of the outputs of some edge detectors operating on a general class of images. In order to analyze the outputs of image operators we must have a statistical characterization of the input image. Often-used assumptions that the intensities or gray levels in an image are independent and identically distributed, or that an image is a sequence of single-parameter processes, are inadequate. An image is inherently a two-dimensional spatial process and hence should be treated as such. The literature in the area of two-dimensional processes is not as rich as in the area of one-dimensional processes. A few spatial processes other than images have received some attention from mathematicians. Examples of such processes that may have some relevance to image processing are the ran-

dom surfaces encountered in sea waves [2], crop yield as a function of spatial location [3], and the height field of a portion of the earth's surface [4]. Fortunately, most of the assumptions made in the analysis of these spatial processes can be reasonably applied to images. Many of these assumptions are necessary for tractability. We shall now summarize the assumptions to be made here regarding the statistical characteristics of the input image.

We assume that the image gray level $z(x,y)$ is a function of the vertical and the horizontal coordinates, x and y. We could also assume that z is a function of time t. This would be important if we were dealing with the dynamic behavior of an image, as in tracking a moving object in a scene. However, we shall be concerned only with static images here, and the dependence of z on t will, therefore, be dropped.

We shall also assume that the parameters x and y and the gray level z itself are continous real variables. Furthermore, it is assumed that the random field can be represented as a sum of periodic functions:

$$z(x,y) = \sum_n a_n \cos (2\pi f_{n,x} x + 2\pi f_{n,y} y + \Theta_n)$$

where $f_{n,x}$ and $f_{n,y}$ are the horizontal and vertical spatial frequencies, a_n is the random amplitude, and Θ_n is the random phase, uniformly distributed in $(0,2\pi)$. By the Central Limit Theorem, $z(x,y)$ is normally distributed and is assumed stationary. The assumption of stationarity implies that the

first and second moments are independent of translation and rotation of the spatial coordinate axes. By imposing this restriction we exclude from further consideration the class of images called context dependent ensembles [5] where specific objects appear at approximately fixed locations. Hunt's example of such an ensemble [5] is the set of facial portraits taken for driver's license photographs, where objects such as the nose, the eyes, etc. appear at approximately the same locations in every picture, and hence, the mean gray level for such an ensemble is definitely a function of the spatial coordinates. In our case, however, we will assume that even if objects occur in our images, they can occur in any positions, and have any orientations, sizes, and shapes.

Thus for the image ensembles that we will be considering, the marginal pdf of the gray level is

$$p(z(x,y)) = \frac{1}{\sqrt{2\pi}\sigma_z} \exp\left[-\frac{(z-\mu_z)^2}{2\sigma_z^2}\right]$$

where μ_z and σ_z are the mean and the standard deviation of $z(x,y)$. Strictly speaking, a normal distribution is inappropriate for image gray level, which is nonnegative. The problem is alleviated if we assume that the mean is much larger than the standard deviation. The value of the mean is, however, irrelevant in many applications, such as determining the autocovariance function of the input image. We shall assume, except when we need certain results explicitly in

terms of μ_z, that the mean has been subtracted from the process $z(x,y)$. We also assume that the autocovariance $R_z(x,y)$ of z and its Fourier transform, the power spectrum $S_z(f_x,f_y)$, have derivatives of all orders required in the analysis.

We define, for later use, the general (i,j)th order moment of a spectral density $S(f_x,f_y)$:

$$m(i,j) = \int_{-\infty}^{\infty} \int_{-\infty}^{\infty} S(f_x,f_y)\ f_x^i\ f_y^j\ df_x\ df_y.$$

In particular, the moments of the input spectral density are

$$m_z(i,j) = \iint S_z(f_x,f_y)\ f_x^i\ f_y^j\ df_x\ df_y.$$

When (i+j) is odd $m_z(i,j)$ is zero for a real process, since the spectral density is even. When (i+j) is even

$$m_z(i,j) = (-1)^{(i+j)/2}\ \frac{\partial^{i+j}}{\partial x^i \partial y^j} R_z(0,0) \qquad (1)$$

The above implies that the moments $m(\cdot)$ satisfy the following relationship:

$$E\left[\frac{\partial^c z}{\partial x^a \partial y^{c-a}} \cdot \frac{\partial^d z}{\partial x^b \partial y^{d-b}}\right] = (-1)^{\frac{d-c}{2}}\ m_z(a+b,(c+d)-(a+b))$$

where a,b,c, and d are positive integers such that c>a, d>b, and c(mod2) = d(mod2) (i.e., c = d±2n, n being an integer). The following is a partial list of the moments for (c+d) ≤ 4:

$$m_z(0,0) = \sigma_z^2$$

$$m_z(2,0) = E\left[\frac{\partial z}{\partial x}\right]^2$$

$$= -E\left[z \cdot \frac{\partial^2 z}{\partial x^2}\right]$$

$$m_z(0,2) = E\left[\frac{\partial z}{\partial y}\right]^2$$

$$= -E\left[z \cdot \frac{\partial^2 z}{\partial y^2}\right]$$

$$m_z(1,1) = E\left[\frac{\partial z}{\partial x} \cdot \frac{\partial z}{\partial y}\right]$$

$$= -E\left[z \cdot \frac{\partial^2 z}{\partial x \partial y}\right]$$

$$m_z(4,0) = E\left[\frac{\partial^2 z}{\partial x^2}\right]^2$$

$$= -E\left[\frac{\partial^3 z}{\partial x^3} \cdot \frac{\partial z}{\partial x}\right]$$

$$= E\left[\frac{\partial^4 z}{\partial x^4}\right]$$

$$m_z(3,1) = E\left[\frac{\partial^2 z}{\partial x \partial y} \cdot \frac{\partial^2 z}{\partial x^2}\right]$$

$$m_z(2,2) = E\left[\frac{\partial^2 z}{\partial x \partial y}\right]^2$$

$$= E\left[\frac{\partial^2 z}{\partial x^2} \cdot \frac{\partial^2 z}{\partial y^2}\right]$$

$$m_z(1,3) = E\left[\frac{\partial^2 z}{\partial x \partial y} \cdot \frac{\partial^2 z}{\partial y^2}\right]$$

$$m_z(0,4) = E\left[\frac{\partial^2 z}{\partial y^2}\right]^2 .$$

2. Edge Detector Responses

In this section we derive expressions for the responses of various basic edge detection operators, including the Laplacian (Section 2.1), absolute Laplacian (Section 2.2), and max of horizontal and vertical absolute differences of average gray levels (Section 2.3).

2.1 Response of the Laplacian

An operator that is used often as an edge detector is the Laplacian operator ∇, given by

$$\nabla = \frac{\partial^2}{\partial x^2} + \frac{\partial^2}{\partial y^2}$$

The edge picture that results when ∇ is applied to the picture $z(x,y)$ is

$$e_1(x,y) = \nabla[z(x,y)]$$

$$= \frac{\partial^2 z}{\partial x^2} + \frac{\partial^2 z}{\partial y^2}$$

Since z is stationary it is easily seen that

$$E[e_1] = 0$$

The cross-covariance function between the image and its edge value is

$$R_{ze_1}(x,y) = \frac{\partial^2}{\partial x^2} R_z(x,y) + \frac{\partial^2}{\partial y^2} R_z(x,y)$$

$$= \nabla(R_z(x,y))$$

Since the autocovariance is a symmetric function, the highest value being at (0,0), it is easily seen that $R_{ze}(0,0) < 0$. The autocovariance function of the edge values is

$$R_{e_1}(x,y) = \frac{\partial^2}{\partial x^2} R_{ze_1}(x,y) + \frac{\partial^2}{\partial y^2} R_{ze_1}(x,y)$$

$$= \nabla^2(R_z(x,y))$$

The density of the local maxima of the edge values can be computed using various moments of the spectral density of the edge value. Let $m_{e_1}(i,j)$ denote the (i,j)th moment of the spectral density $S_{e_1}(f_x,f_y)$ of the edge value. Let

$$M_2 = \begin{bmatrix} m_{e_1}(2,0) & m_{e_1}(1,1) \\ m_{e_1}(1,1) & m_{e_1}(0,2) \end{bmatrix}$$

and

$$M_4 = \begin{bmatrix} m_{e_1}(4,0) & m_{e_1}(3,1) & m_{e_1}(2,2) \\ m_{e_1}(3,1) & m_{e_1}(2,2) & m_{e_1}(1,3) \\ m_{e_1}(2,2) & m_{e_1}(1,3) & m_{e_1}(0,4) \end{bmatrix}$$

and $\ell_1 \geq \ell_2 \geq \ell_3$ be the three eigenvalues of the matrix product

$$M_4 \cdot \begin{bmatrix} 0 & 0 & 1/2 \\ 0 & -1 & 0 \\ 1/2 & 0 & 0 \end{bmatrix} . \qquad (2)$$

Then the density of local maxima of edge value is (see [2])

$$D(e_1) = \frac{1}{2\pi^2} \frac{\ell_1}{|M_2|^{\frac{1}{2}}} \left[\left(\frac{\ell_2 \ell_3}{\ell_1^2} \right)^{\frac{1}{2}} \left\{ \left(\frac{\ell_2 - \ell_1}{\ell_2} \right)^{\frac{1}{2}} F_1(k) - \left(\frac{\ell_2}{\ell_2 - \ell_1} \right)^{\frac{1}{2}} F_2(k) \right\} \right] \qquad (3)$$

where

$$|M_2| = \det(M_2)$$

$$k^2 = \frac{\ell_1(\ell_3 - \ell_2)}{\ell_3(\ell_1 - \ell_2)}$$

and F_1 and F_2 are the Legendre elliptic integrals of the first and second kind:

$$F_1(k) = \int_0^{\pi/2} (1 - k^2 \sin^2\theta)^{\frac{1}{2}} \, d\theta$$

$$F_2(k) = \int_0^{\pi/2} (1 - k^2 \sin^2\theta)^{-\frac{1}{2}} \, d\theta \ .$$

Taking the determinant of the appropriate matrix we find that the three eigenvalues are given by the solution of the cubic equation

$$4\ell^3 - 3A\ell - |M_4| = 0$$

where

$$A = \frac{1}{3} m_{e_1}(4,0) m_{e_1}(0,4) - \frac{4}{3} m_{e_1}(3,1) m_{e_1}(1,3) + m_{e_1}^2(2,2)$$

From the matrix product (2) it can be shown that [2]

$$\ell_1 + \ell_2 + \ell_3 = 0$$

$$\ell_1 \ell_2 \ell_3 > 0 \ .$$

The quantity in the square brackets in eqn. (3) departs very little from unity throughout its range [2], yielding

$$D(e_1) \simeq \frac{\ell_1}{2\pi^2 |M_2|^{\frac{1}{2}}} \cdot$$

If the edge response is isotropic we have $m_{e_1}(i,j) = 0$ when i or j is odd [6] and

$$\ell_1 = -2\ell_2$$

$$\ell_2 = \ell_3$$

$$\ell_1 = \frac{2}{3} m_{e_1}(4,0) \cdot$$

Thus eqn. (3) reduces to

$$D(e_1) = \frac{1}{2\pi^2} \cdot \frac{2\, m_{e_1}(4,0)}{3\, m_{e_1}(2,0)} \cdot \frac{\pi}{2\sqrt{3}}$$

$$= \frac{m_{e_1}(4,0)}{6\sqrt{3}\,\pi\, m_{e_1}(2,0)} \cdot \qquad (4)$$

2.2 Response of the Absolute Laplacian

Let $e_2(x,y) = |\nabla z(x,y)|$

$$= \left| \frac{\partial^2 z}{\partial x^2} + \frac{\partial^2 z}{\partial y^2} \right|$$

Whereas $e_1(x,y)$ was Gaussian, $e_2(x,y)$ is not Gaussian. The mean value of e_2 can be easily found to be

$$E[e_2(x,y)] = \sqrt{\frac{2}{\pi} m_{e_1}(0,0)} \tag{5a}$$

$$= \sqrt{\frac{2}{\pi} \nabla^2 R_z(0,0)} \tag{5b}$$

since $e_2 = |e_1|$. Using Price's theorem for nonlinear systems with Gaussian inputs [7,8] we obtain

$$\frac{\partial}{\partial \nu} R_{ze_2}(x,y) = \frac{\partial}{\partial \nu} E[z(\alpha,\beta)|e_1(\alpha+x,\beta+y)|]$$

$$= E\left[\frac{\partial^2 z(\alpha,\beta)|e_1(\alpha+x,\beta+y)|}{\partial z(\alpha,\beta)\partial e_1(\alpha+x,\beta+y)}\right] \tag{6}$$

where

$$\nu = E[z(\alpha,\beta)e_1(\alpha+x,\beta+y)]$$

$$= R_{ze_1}(x,y) .$$

The derivative in square brackets in eqn. (6) is

$$[\cdot] = 1 \text{ if } e_1(\cdot) > 0$$

$$-1 \text{ if } e_1(\cdot) < 0$$

from which it follows that

$$E[\cdot] = Pr\{e_1(\cdot) > 0\} - Pr\{e_1(\cdot) < 0\}$$

$$= 0 \tag{7}$$

since $e_1(x,y)$ is zero-mean Gaussian. Substituting eqn. (7) in eqn. (6) we get

$$R_{ze_2}(x,y) = \int_{-\infty}^{\nu} E[\cdot]\, d\nu$$

$$= \int_{-\infty}^{\nu} 0\, d\nu$$

$$= 0 \tag{8}$$

Therefore, unlike the Laplacian, the absolute Laplacian at a point is uncorrelated with the gray level at any point. Similarly, using Price's theorem it can be shown that the auto-covariance function of the absolute Laplacian response is

$$R_{e_2}(x,y) = E[e_2(\alpha,\beta)e_2(x+\alpha,y+\beta)] - E^2[e_2(\alpha,\beta)]$$

$$= E[|e_1(\alpha,\beta)||e_1(x+\alpha,y+\beta)|] - \frac{2}{\pi} m_{e_1}(0,0)$$

$$= \frac{2}{\pi} m_{e_1}(0,0)[\cos\theta + \theta\sin\theta - 1] \tag{9}$$

where $\theta = \sin^{-1} \frac{R_{e_1}(x,y)}{R_{e_1}(0,0)}$, $-\frac{\pi}{2} < \theta \leq \frac{\pi}{2}$.

Computing the density of local maxima of the absolute Laplacian is formidable. But an approximate result can be obtained if one assumes that the probability of a local maximum Laplacian being negative, or of a local minimum Laplacian being positive, is negligibly small*. Under this assumption the density of local maxima of the absolute Laplacian is twice that of the Laplacian:

$$D(e_2) = 2D(e_1) \tag{10}$$

where we use the fact that the density of local minima of the Laplacian is the same as that of its local maxima [2].

---

*For a narrow spectrum the height of a local maximum Gaussian function has been shown to be nonnegative [2].

2.3 Response of the DIFF Operator

DIFF is an edge operator, defined for discretized images, which incorporates a local neighborhood smoothing into the edge detection [9] to reduce its sensitivity to noise. The analog of the operator for continuous domain images may be described as follows. Let $e_3(x,y)$ be the response at (x,y) of the DIFF operator that performs smoothing of noise over a kxk square window. Then, by definition

$$e_3 = \max[|e_{4x}|, |e_{4y}|]$$

$$e_{4x} = [z(x+\tfrac{k}{2},y) \bullet \text{Rect}\ (\tfrac{x}{k}, \tfrac{y}{k})] - [z(x-\tfrac{k}{2},y) \bullet \text{Rect}\ (\tfrac{x}{k}, \tfrac{y}{k})]$$

$$e_{4y} = [z(x,y+\tfrac{k}{2}) \bullet \text{Rect}\ (\tfrac{x}{k}, \tfrac{y}{k})] - [z(x,y-\tfrac{k}{2}) \bullet \text{Rect}\ (\tfrac{x}{k}, \tfrac{y}{k})]$$

where

$$\text{Rect}(\tfrac{x}{k}, \tfrac{y}{k}) = \begin{cases} \frac{1}{k^2} & |\tfrac{x}{k}| \le \tfrac{1}{2},\ |\tfrac{y}{k}| \le \tfrac{1}{2} \\ 0 & \text{elsewhere.} \end{cases}$$

Here $\bullet$ denotes convolution and the functions e_3, e_{4x}, and e_{4y} are functions of (x,y). If we define

$$s(x,y) = z(x,y) \bullet \text{Rect}\ (\tfrac{x}{k}, \tfrac{y}{k})$$

then

$$e_{4x} = s(x+\tfrac{k}{2},y) - s(x-\tfrac{k}{2},y)$$

$$e_{4y} = s(x,y+\tfrac{k}{2}) - s(x,y-\tfrac{k}{2}).$$

The mean edge value is

$$E[e_3] = E[\max\{|e_{4x}|, |e_{4y}|\}],$$

Let $E[e_{4x} \cdot e_{4y}] = \alpha$. Using McMahon's theorem [10] we have

$$\frac{\partial}{\partial\alpha} E[e_3] = E\left[\frac{\partial^2}{\partial e_{4x}\partial e_{4y}} \max\{|e_{4x}|, |e_{4y}|\}\right]$$

$$= E[\delta(e_{4x}+e_{4y}) - \delta(e_{4x}-e_{4y})]$$

$$= Pr(e_{4x} = -e_{4y}) - Pr(e_{4x} = e_{4y})$$

Using the appropriate joint normal pdf's for e_{4x} and e_{4y} we obtain

$$\frac{\partial}{\partial\alpha} E[e_3] = \frac{1}{\sqrt{2\pi}}\left[\frac{1}{\sqrt{\sigma_x^2+\sigma_y^2+2\alpha}} - \frac{1}{\sqrt{\sigma_x^2+\sigma_y^2-2\alpha}}\right]$$

where $\sigma_x^2 = E[e_{4x}^2]$, $\sigma_y^2 = E[e_{4y}^2]$.

Therefore

$$E[e_3] = \frac{1}{\sqrt{2\pi}} \int_0^{\alpha}\left[\frac{1}{\sqrt{\sigma_x^2+\sigma_y^2+2\alpha}} - \frac{1}{\sqrt{\sigma_x^2+\sigma_y^2-2\alpha}}\right] d\alpha + E[e_3|\alpha=0]$$

$$= \frac{1}{\sqrt{2\pi}}\left[\sqrt{\sigma_x^2+\sigma_y^2+2\alpha}\Big|_0^{\alpha} - \sqrt{\sigma_x^2+\sigma_y^2-2\alpha}\Big|_0^{\alpha}\right] + E[e_3|\alpha=0]$$

$$= \frac{1}{\sqrt{2\pi}}\left[\sqrt{\sigma_x^2+\sigma_y^2+2\alpha} + \sqrt{\sigma_x^2+\sigma_y^2-2\alpha} - 2\sqrt{\sigma_x^2+\sigma_y^2}\right] + E[e_3|\alpha=0] \quad (11)$$

Equation (11) implies that as the magnitude of the correlation between the horizontal difference e_{4x} and vertical difference e_{4y} increases the average value of e_3 decreases. $E[e_3|\alpha = 0]$ can be obtained as follows: Let

$$|e_{4x}| = \beta$$

$$|e_{4y}| = \gamma.$$

The marginal pdf's of β and γ are

$$p(\beta) = \frac{2}{\sqrt{2\pi}\sigma_x} \exp(-\frac{\beta^2}{2\sigma_x^2})U(\beta)$$

$$p(\gamma) = \frac{2}{\sqrt{2\pi}\sigma_y} \exp(-\frac{\gamma^2}{2\sigma_y^2})U(\gamma)$$

When α is zero, e_{4x} and e_{4y} are independent and, therefore, β and γ are also independent. The pdf of $e_3 = \max(\beta,\gamma)$ can be easily found to be

$$p(e_3) = [p(\beta)\ P(\gamma) + p(\gamma)\ P(\beta)]\Big|_{\substack{\beta=e_3 \\ \gamma=e_3}}$$

In terms of the normal distribution function φ, $P(\beta)$ and $P(\gamma)$ are given by

$$P(\beta) = 2\varphi(\beta/\sigma_x) - 1$$

$$P(\gamma) = 2\varphi(\gamma/\sigma_y) - 1$$

where $\varphi(\cdot) = \int_{-\infty}^{(\cdot)} \frac{1}{\sqrt{2\pi}} \exp(-\xi^2/2)d\xi.$

The quantity α may be determined as follows:

$$\begin{aligned}\alpha &= E[e_{4x}\ e_{4y}] \\ &= E[\{s(x,y+\tfrac{k}{2}) - s(x,y-\tfrac{k}{2})\}\{s(x+\tfrac{k}{2},y) - s(x-\tfrac{k}{2},y)\}] \\ &= 2[R_s(\tfrac{k}{2}, -\tfrac{k}{2}) - R_s(\tfrac{k}{2}, \tfrac{k}{2})]\end{aligned}$$

$$= 2[R_z(\tfrac{k}{2}, -\tfrac{k}{2}) - R_z(\tfrac{k}{2}, \tfrac{k}{2})] \bullet \mathrm{Rect}(\tfrac{x}{k}, \tfrac{y}{k}) \bullet \mathrm{Rect}(\tfrac{x}{k}, \tfrac{y}{k})$$

When α is not zero the pdf of e_3 can be shown to be

$$p(e_3) = \int_{-\infty}^{e_3} p(\beta, e_3)\, d\beta + \int_{-\infty}^{e_3} p(e_3, \gamma)\, d\gamma \qquad (12)$$

where $p(\cdot,\cdot)$ is the joint pdf of β and γ. Letting

$\kappa = \alpha/(\sigma_x\sigma_y)$, the joint pdf is given by

$$p(\beta,\gamma) = \frac{1}{\pi\sigma_x\sigma_y\sqrt{(1-\kappa^2)}} \left[\exp\left\{-\frac{1}{2(1-\kappa^2)}\left(\frac{\beta^2}{\sigma_x^2} - \frac{2\kappa\beta\gamma}{\sigma_x\sigma_y} + \frac{\gamma^2}{\sigma_y^2}\right)\right\}\right.$$

$$\left. + \exp\left\{-\frac{1}{2(1-\kappa^2)}\left(\frac{\beta^2}{\sigma_x^2} + \frac{2\kappa\beta\gamma}{\sigma_x\sigma_y} + \frac{\gamma^2}{\sigma_y^2}\right)\right\}\right] U(\beta)U(\gamma)\ .$$

The average value of e_3 may also be found using eqn. (12).

Following the derivations that led to eqn. (8) it may be seen that the gray level $z(x,y)$ at a point (x,y) is uncorrelated with $\beta(x',y')$ and $\gamma(x',y')$ at any point (x',y'). From this it follows that $z(x,y)$ is also uncorrelated with $\max[\beta(x',y'), \gamma(x',y')]$, i.e., with the edge value $e_3(x',y')$. Computing the autocovariance function of $e_3(x,y)$ seems to be a difficult task.

We shall determine an approximate density of local maxima of $e_3(x,y)$ in the following way. The densities $D(e_{4x})$ and $D(e_{4y})$ of local maxima of e_{4x} and e_{4y}, respectively, can be obtained by using eqn. (4). The eigenvalues ℓ_1, ℓ_2, and ℓ_3 are different from those used in evaluating $D(e_1)$, obviously. The density $D(\beta)$ of local maxima of β is assumed to be related to $D(e_{4x})$ in the same way that $D(e_2)$ (see eqn. (10)) is related to $D(e_1)$. The same argument also holds for $D(\gamma)$, the density of local maxima of γ, and $D(e_{4y})$. Now the density of local maxima of e_3 is

$$D(e_3) = D(\beta)\ Pr(\beta>\gamma) + D(\gamma)\ Pr(\gamma>\beta)$$

where $Pr(\beta>\gamma)$ is the probability of a horizontal edge and $Pr(\gamma>\beta) = 1 - Pr(\beta>\gamma)$ is the probability of a vertical edge.

3. Responses for a Class of Synthetic Images

It is desirable to examine how well the theoretical results given in Section 2 can predict various statistical properties of edge responses to actual image data. In testing formulas on actual image data it should be borne in mind that the accuracy of the predicted quantities depends on two things: how accurately the power spectrum used to evaluate the predicted quantities models the image data, and how accurately the image satisfies some of the assumptions made in deriving the predicted quantities. Some of the important assumptions made in the derivations are that

i) the gray levels of the input images and the edge pictures are continuous valued,

ii) the input images are stationary with normally distributed gray levels,

iii) the input images and the edge pictures are random fields with continuous parameters (spatial coordinates).

In some cases it was further assumed that

iv) the covariance functions are isotropic.

These constraints are imposed for reasons of tractability. Some of them may not be satisfied by real images. Thus, errors in the predicted quantities may be due to violation of any of the assumptions above, or due to the use of an inappropriate power spectrum (or autocovariance function) for the image data. The problem of selecting an appropriate autocovariance function for the available image data is a separate research area. We shall experiment with images that

are discretized and quantized, thus violating some of the assumptions listed above, but that have power spectra that are known a priori. We obtain test image data with known power spectra by using synthetic images.

A class of power spectra that is often used to model images and can be easily achieved in synthetic discrete images is the class corresponding to a separable exponential autocovariance function. These synthetic images can be generated in a computer by using normally distributed pseudorandom numbers and the following expression:

$$z(x,y) = \rho_1 z(x-1,y) + \rho_2 z(x,y-1) - \rho_1\rho_2 z(x-1,y-1) + \omega(x,y) + \mu_z \qquad (13)$$

where x and y are assumed to be discrete valued, $\omega(x,y)$ is a sequence of normally distributed zero mean pseudorandom numbers with variance $(1-\rho_1^2)(1-\rho_2^2)m_z(0,0)$, and ρ_1 and ρ_2 are two parameters such that $0 \leq \rho_1, \rho_2 \leq 1$. The mean and variance of the image should be so chosen that the probability of a gray level generated by eqn. (13) being outside the image grayscale becomes very small. This reasonably assures a normal distribution of the image gray level. Unfortunately, the power spectrum of image generated by eqn. (13) cannot be made isotropic. The problem may be partially alleviated by choosing $\rho_1 = \rho_2 = \rho$, making the spectrum identical in any two orthogonal directions, such as the horizontal and the vertical directions. In the sequel such a power spectrum will

be assumed. Various estimators derived in the last section will now be evaluated for this power spectrum.

3.1 The Laplacian

The cross-covariance function between the image and its discrete Laplacian is

$$R_{ze_1}(x,y) = \nabla[R_z(x,y)]$$

$$= R_z(x,y) \bullet \begin{bmatrix} 0 & 1 & 0 \\ 1 & -4 & 1 \\ 0 & 1 & 0 \end{bmatrix} \quad * \tag{14}$$

where $\bullet$ is discrete convolution, and for the test images

$$R_z(x,y) = m_z(0,0)\ \rho^{|x| + |y|}. \tag{15}$$

Similarly,

$$R_{e_1}(x,y) = R_z(x,y) \bullet \begin{bmatrix} 0 & 0 & 1 & 0 & 0 \\ 0 & 2 & -8 & 2 & 0 \\ 1 & -8 & 20 & -8 & 1 \\ 0 & 2 & -8 & 2 & 0 \\ 0 & 0 & 1 & 0 & 0 \end{bmatrix} \tag{16}$$

Specifically, the variance of e_1 is

$$m_{e_1}(0,0) = R_{e_1}(0,0)$$

$$= m_z(0,0)[20-32\rho+12\rho^2]. \tag{17}$$

The covariance coefficient between the Laplacian at two horizontal neighbors is

---

*This matrix representation of a two-dimensional discrete function shows the value of the function around the origin. The origin corresponds to the center of the matrix. Values of the function not shown in the matrix are zero.

$$\rho_{he_1} = \frac{R_{e_1}(1,0)}{m_{e_1}(0,0)}$$

$$= \frac{[-8 + 25\rho - 24\rho^2 + 7\rho^3]}{[20 - 32\rho + 12\rho^2]} .$$

The vertical covariance coefficient ρ_{ve_1} is the same as ρ_{he_1}.

The diagonal covariance coefficient of the Laplacian response is given by

$$\rho_{de_1} = \frac{R_{e_1}(1,1)}{m_{e_1}(0,0)}$$

$$= \frac{2 - 16\rho + 26\rho^2 - 16\rho^3 + 4\rho^4}{20 - 32\rho + 12\rho^2} .$$

The cross-covariance coefficient between the gray level and the Laplacian at a point is

$$\Psi_{e_1} = \frac{R_{ze_1}(0,0)}{\sqrt{m_z(0,0)m_{e_1}(0,0)}}$$

$$= \frac{4(-1+\rho)}{\sqrt{20 - 32\rho + 12\rho^2}}$$

The horizontal (or vertical) and diagonal cross-covariance coefficients are given, respectively, by

$$\psi_{he_1} = \psi_{ve_1} = \frac{R_{ze_1}(1,0)}{\sqrt{m_z(0,0)m_{e_1}(0,0)}}$$

$$= \frac{1-4\rho + 3\rho^2}{\sqrt{20 - 32\rho + 12\rho^2}}$$

$$\psi_{de_1} = \frac{R_{ze_1}(1,1)}{\sqrt{m_z(0,0)m_{e_1}(0,0)}}$$

$$= \frac{\rho(1-2\rho+\rho^2)}{\sqrt{5 - 8\rho + 3\rho^2}}$$

Using eqn. (1) we can obtain the necessary moments of the spectral density to determine the density of the local maxima of the edge responses. However, determining the necessary eigenvalues in terms of ρ is very cumbersome. We shall approximate the density of local maxima by

$$D(e_1) \approx \frac{m_{e_1}(4,0)}{6\sqrt{3}\pi m_{e_1}(2,0)} \quad .$$

In other words, we approximate the density by that of an edge response which is isotropic Gaussian with the same second moment m(2,0) and fourth moment m(4,0) as the Laplacian. The two necessary moments can be computed from the autocovariance function by

$$m_{e_1}(2,0) = - \frac{\partial^2 R_{e_1}(0,0)}{\partial x^2}$$

$$m_{e_1}(4,0) = \frac{\partial^4 R_{e_1}(0,0)}{\partial x^4} .$$

Substituting the appropriate expressions from eqn. (16) we get

$$m_{e_1}(2,0) = 2R_{e_1}(0,0) - 2R_{e_1}(1,0)$$

$$= 2[20 - 32\rho + 12\rho^2 - (-8 + 25\rho - 24\rho^2 + 7\rho^3)]$$

$$= 56 - 114\rho + 72\rho^2 - 14\rho^3$$

$$m_{e_1}(4,0) = 6R_{e_1}(0,0) - 8R_{e_1}(1,0) + 2R_{e_1}(2,0)$$

$$= 6(20 - 32\rho + 12\rho^2)$$

$$-8(-8 + 25\rho - 24\rho^2 + 7\rho^3)$$

$$+2(1 - 8\rho + 24\rho^2 - 24\rho^3 + 7\rho^4)$$

$$= 186 - 408\rho + 312\rho^2 - 104\rho^3 + 14\rho^4.$$

Thus,

$$D(e_1) \approx \frac{93 - 204\rho + 156\rho^2 - 52\rho^3 + 7\rho^4}{6\sqrt{3}\pi[28 - 57\rho + 36\rho^2 - 7\rho^3]} \qquad (18)$$

which is independent of the image variance $m_z(0,0)$.

3.2 The Absolute Laplacian

The average absolute Laplacian is, from eqns. (5a) and (17),

$$E\{e_2(x-y)\} = \frac{2}{\pi} m_z(0,0)[20 - 32\rho + 12\rho^2].$$

From eqn. (9)

$$\begin{aligned} Var(e_2) &= m_{e_1}(0,0)\ [1 - \tfrac{2}{\pi}] \\ &= \tfrac{\pi-2}{\pi} m_z(0,0)\ [20 - 32\rho + 12\rho^2]. \\ &= \tfrac{\pi-2}{\pi} Var(e_1). \end{aligned}$$

The horizontal (or vertical) and diagonal autocovariance coefficients are, using eqn. (9),

$$\rho_{he_2} = \rho_{ve_2} = \frac{2(\cos\theta_h + \theta_h \sin\theta_h - 1)}{\pi - 2}$$

$$\rho_{de_2} = \frac{2(\cos\theta_d + \theta_d \sin\theta_d - 1)}{\pi - 2}$$

where $\theta_h = \sin^{-1}\rho_{he_1}$ and $\theta_d = \sin^{-1}\rho_{de_1}$. The density of the absolute Laplacian local maxima is approximated, following eqns. (18) and (10), by

$$D(e_2) \approx \frac{93 - 204\rho + 156\rho^2 + 52\rho^3 + 7\rho^4}{3\sqrt{3}\,\pi\,[28 - 57\rho + 36\rho^2 - 7\rho^3}\ .$$

3.3 The DIFF Operator

We shall now evaluate some statistical properties of the edge response when the DIFF operator is used as the edge detector. For the 2x2 DIFF operator, s(x,y) (see Section 2.3 for the definition of s(x,y)) and $R_s(x,y)$ are as follows:

$$s(x,y) = \frac{1}{4}\, z(x,y) \bullet \begin{bmatrix} 0 & 0 & 0 \\ 0 & 1 & 1 \\ 0 & 1 & 1 \end{bmatrix}$$

$$R_s(x,y) = \frac{1}{16}\, R_z(x,y) \bullet \begin{bmatrix} 0 & 0 & 0 \\ 0 & 1 & 1 \\ 0 & 1 & 1 \end{bmatrix} \bullet \begin{bmatrix} 1 & 1 & 0 \\ 1 & 1 & 0 \\ 0 & 0 & 0 \end{bmatrix}$$

$$= \frac{1}{16}\, R_z(x,y) \bullet \begin{bmatrix} 1 & 2 & 1 \\ 2 & 4 & 2 \\ 1 & 2 & 1 \end{bmatrix}$$

Specifically,

$$R_s(0,0) = \frac{m_z(0,0)}{16}\,[4 + 8\rho + 4\rho^2]$$

$$R_s(0,2) = R_s(2,0)$$

$$= \frac{m_z(2,0)}{16}\,[2\rho + 6\rho^2 + 6\rho^3 + 2\rho^4]$$

$$= \frac{m_z(0,0)}{16}\,[1 + 4\rho + 6\rho^2 + 4\rho^3 + 4\rho^4]$$

from which it follows that the correlation α (see Section 2.3) between e_{4x} and e_{4y} is zero. It may be noted that for an image where $R_z(x,y) \neq R_z(-x,y)$, as, for example, in an image with more correlation in one diagonal direction than in the other, α may not necessarily be zero. The variances σ_x^2 and σ_y^2

are equal and

$$\sigma_x^2 = E[e_{4x}^2]$$

$$= E[\{s(x+1,y) - s(x-1,y)\}^2]$$

$$= 2R_s(0,0) - 2R_s(2,0)$$

$$= \frac{m_z(0,0)}{4}\,[2 + 3\rho - \rho^2 - 3\rho^3 - \rho^4] \ .$$

For a completely correlated image ($\rho=1$) this variance is zero and for a completely uncorrelated image ($\rho=0$) this variance is one half of the image variance. From Section 2.3 we have

$$p(e_3) = \frac{4}{\sqrt{2\pi}\,\sigma_x} \exp\left(-\frac{e_3^2}{2\sigma_x^2}\right)\left[2\varphi\left(\frac{e_3}{\sigma_x}\right) - 1\right]U(e_3) \ . \qquad (19)$$

For a given $m_z(0,0)$ and ρ this density can be used to evaluate $E[e_3]$. Performing the necessary integrations yields a very simple expression for $E[e_3]$ as follows:

$$E[e_3] = \int_0^\infty e_3 \frac{4}{\sqrt{2\pi}\sigma_x}\left[\exp\left(-\frac{e_3^2}{2\sigma_x^2}\right)\right] 2\int_0^{e_3} \frac{1}{\sqrt{2\pi}\sigma_x} \exp -\left(\frac{\xi^2}{2\sigma_x^2}\right) d\xi de_3$$

$$= \frac{8\sigma_x}{2\pi} \int_0^\infty \int_0^u u \exp\left(-\frac{u^2+v^2}{2}\right) dvdu \quad \text{(by substituting } u = \frac{e_3}{\sigma_x} \text{ and } v = \frac{\xi}{\sigma_x}\text{)}$$

$$= \frac{4\sigma_x}{\pi} \int_0^\infty \int_0^{\pi/4} r\cos\theta \exp\left(-\frac{r^2}{2}\right) r\,d\theta\,dr \quad \text{(using polar coordinates)}$$

$$= \frac{4\sigma_x}{\pi} \int_0^{\pi/4} \cos\theta d\theta \int_0^{\infty} r^2 \exp - \frac{r^2}{2}\, dr$$

$$= \frac{2\sigma_x}{\sqrt{\pi}} \quad .$$

By using the same method we find that

$$E[e_3^2] = \frac{\pi+2}{\pi} \sigma_x^2 \ ,$$

from which the variance of the edge response is

$$\mathrm{Var}(e_3) = E[e_3^2] - E^2[e_3]$$

$$= \sigma_x^2 [\frac{\pi+2}{\pi} - \frac{4}{\pi}]$$

$$= \frac{\pi-2}{\pi} \sigma_x^2 \quad .$$

The density of local maxima of e_{4x} is, using a similar approximation as for $D(e_1)$,

$$D(e_{4x}) \approx \frac{6R_{e_{4x}}(0,0) - 8R_{e_{4x}}(1,0) + 2R_{e_{4x}}(2,0)}{12\sqrt{3}\,\pi\,[R_{e_{4x}}(0,0) - R_{e_{4x}}(1,0)]} \quad .$$

Due to symmetry in $R_z(x,y)$ we have $D(e_{4x}) = D(e_{4y})$. If we assume that $\Pr(|e_{4x}|>|e_{4y}|) = \Pr(|e_{4y}|>|e_{4x}|)$ then, from Section 2.3,

$$D(e_3) \approx 2D(e_{4x})$$

$$= \frac{3R_{e_{4x}}(0,0) - 4R_{e_{4x}}(1,0) + 2R_{e_{4x}}(2,0)}{3\sqrt{3}\,\pi\,[R_{e_{4x}}(0,0) - R_{e_{4x}}(1,0)]} \quad . \qquad (20)$$

Since

$$e_{4x}(x,y) = s(x,y) \bullet [1 \quad 0 \quad -1]$$

$$R_{e_{4x}}(x,y) = R_s(x,y) \bullet [-1\ 0\ 2\ 0\ -1]$$

$$= \frac{1}{16} R_z(x,y) \bullet \begin{bmatrix} -1 & -2 & 1 & 4 & 1 & -2 & -1 \\ -2 & -4 & 2 & 8 & 2 & -4 & -2 \\ -1 & -2 & 1 & 4 & 1 & -2 & -1 \end{bmatrix} .$$

Thus

$$R_{e_{4x}}(0,0) = \frac{m_z(0,0)}{16} [8 + 12\rho - 4\rho^2 - 12\rho^3 - 4\rho^4]$$

$$R_{e_{4x}}(1,0) = \frac{m_z(0,0)}{16} [2 + 6\rho + 4\rho^2 - 4\rho^3 - 6\rho^4 - 2\rho^5]$$

$$R_{e_{4x}}(2,0) = \frac{m_z(0,0)}{16} [-4-4\rho + 8\rho^2 + 10\rho^3 - 2\rho^4 - 2\rho^6] .$$

Substituting these results in eqn. (20) and simplifying yields the surprisingly simple result

$$D(e_3) \simeq \frac{2(2 - \rho + \rho^3)}{3\sqrt{3}\,\pi\,(3-\rho^2)} .$$

For the 4x4 DIFF operator the value of α is zero, just as it is for the 2x2 DIFF operator. The variances σ_x^2 and σ_y^2 are also equal and

$$\sigma_x^2 = E[\{s(x+2,y) - s(x-2,y)\}^2]$$

$$= 2[R_s(0,0) - R_s(4,0)] .$$

Now,

$$s(x,y) = \frac{1}{16}\, z(x,y) \bullet \begin{bmatrix} 0 & 0 & 0 & 0 & 0 \\ 0 & 1 & 1 & 1 & 1 \\ 0 & 1 & 1 & 1 & 1 \\ 0 & 1 & 1 & 1 & 1 \\ 0 & 1 & 1 & 1 & 1 \end{bmatrix}$$

$$R_s(x,y) = \frac{1}{256}\, R_z(x,y) \bullet \begin{bmatrix} 0 & 0 & 0 & 0 & 0 \\ 0 & 1 & 1 & 1 & 1 \\ 0 & 1 & 1 & 1 & 1 \\ 0 & 1 & 1 & 1 & 1 \\ 0 & 1 & 1 & 1 & 1 \end{bmatrix} \bullet \begin{bmatrix} 1 & 1 & 1 & 1 & 0 \\ 1 & 1 & 1 & 1 & 0 \\ 1 & 1 & 1 & 1 & 0 \\ 1 & 1 & 1 & 1 & 0 \\ 0 & 0 & 0 & 0 & 0 \end{bmatrix}$$

$$= \frac{1}{256}\, R_z(x,y) \bullet \begin{bmatrix} 1 & 2 & 3 & 4 & 3 & 2 & 1 \\ 2 & 4 & 6 & 8 & 6 & 4 & 2 \\ 3 & 6 & 9 & 12 & 9 & 6 & 3 \\ 4 & 8 & 12 & 16 & 12 & 8 & 4 \\ 3 & 6 & 9 & 12 & 9 & 6 & 3 \\ 2 & 4 & 6 & 8 & 6 & 4 & 2 \\ 1 & 2 & 3 & 4 & 3 & 2 & 1 \end{bmatrix} .$$

We obtain, using the above expression,

$$\sigma_x^2 = \frac{m_z(0,0)}{64}\,[8 + 22\rho + 27\rho^2 + 18\rho^3 - 2\rho^4 - 18\rho^5 - 22\rho^6 - 18\rho^7 - 10\rho^8 - 4\rho^9 - \rho^{10}] .$$

As in the case of 2x2 DIFF we can compute the density $D(e_3)$ in terms of σ_x^2. But the computation of the density of local maxima is more tedious in the case of 4x4 DIFF than in the case of 2x2 DIFF and will not be attempted.

4. Experimental Evaluation

A set of 64x64 test images was generated using eqn. (13) with various values of the correlation coefficient $\rho(= \rho_1 = \rho_2)$ and variance $m_z(0,0)$. The image grayscale was 0 to 63 and the mean μ_z was set to 31. The highest value of the moment $m_z(0,0)$ was 100, so that the probability of a gray level being outside the range of 0 to 63 was less than 0.2%. Specifically, the test images had $m_z(0,0)$ = 5, 10, 15, 20, 30, 40, 50, 60, 70, 80, 90, and 100, and for each value of $m_z(0,0)$ there were four test images, with ρ = 0.6, 0.65, 0.7, and 0.75, thus giving 48 images in total. The test images are shown in Figure 1. Two samples of the histograms of the test images are shown in Figure 2.

The responses of the Laplacian, the absolute Laplacian , the 2x2 DIFF and the 4x4 DIFF operators to each of the test images were computed. Various statistical properties were estimated* from these "response pictures" and plotted as functions of the input variance or the input correlation coefficient. Similar graphs of the predicted quantities were also made and compared with the estimated values. Figures 3 to 6 show the graphs. In some of the figures only one or two samples of the estimated functions are shown to avoid overcrowding due to the noisy nature of the estimated functions.

---

*The ensemble average was substituted by the sample mean to obtain the estimators.

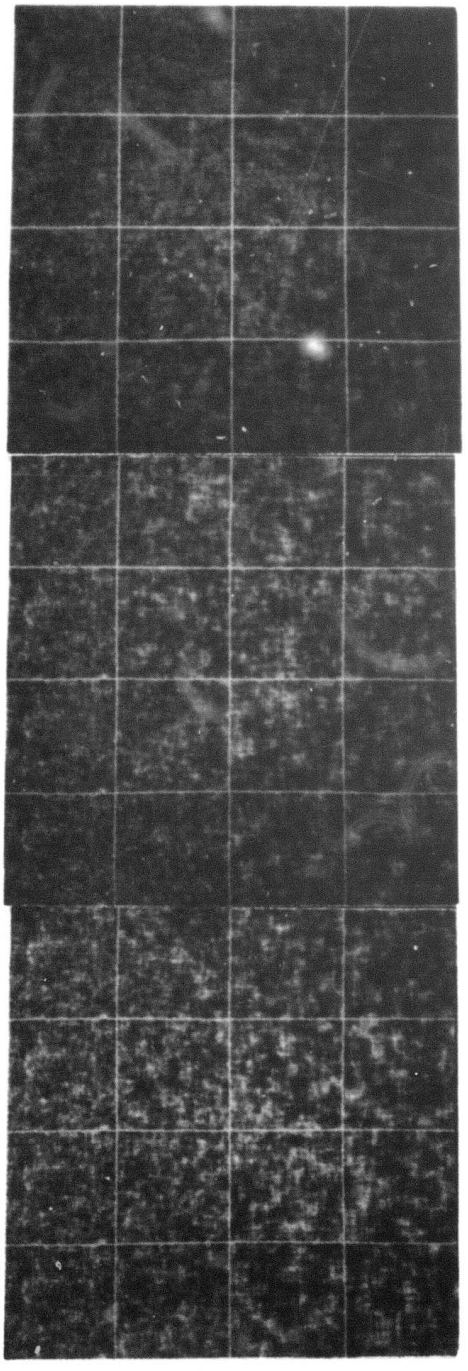

Figure 1. The 48 test images, arranged with increasing variance from top to bottom and increasing correlation from left to right.

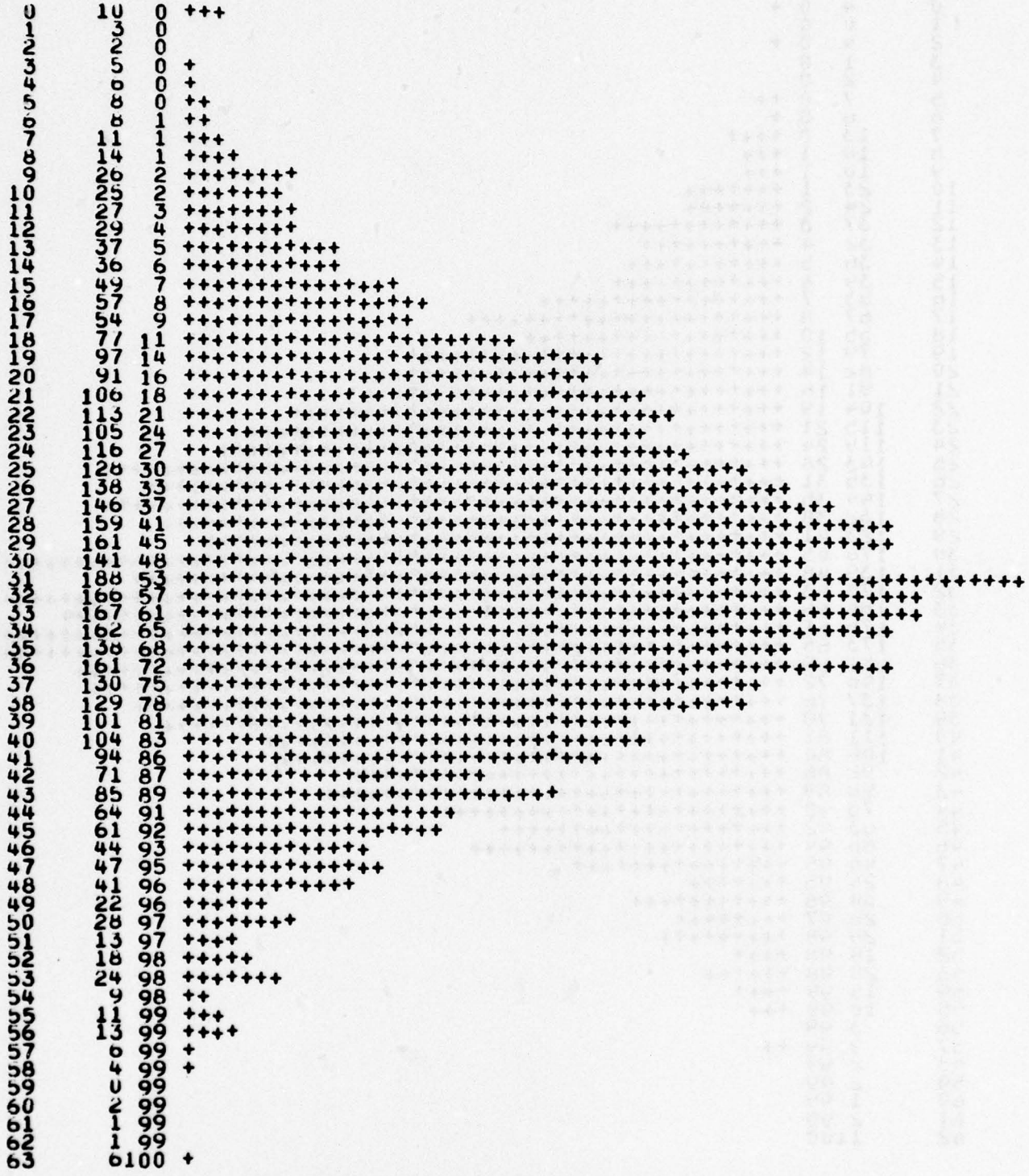

Figure 2. The histograms of two of the test images, with $m_z(0,0) = 100$.

a. $\rho = 0.6$

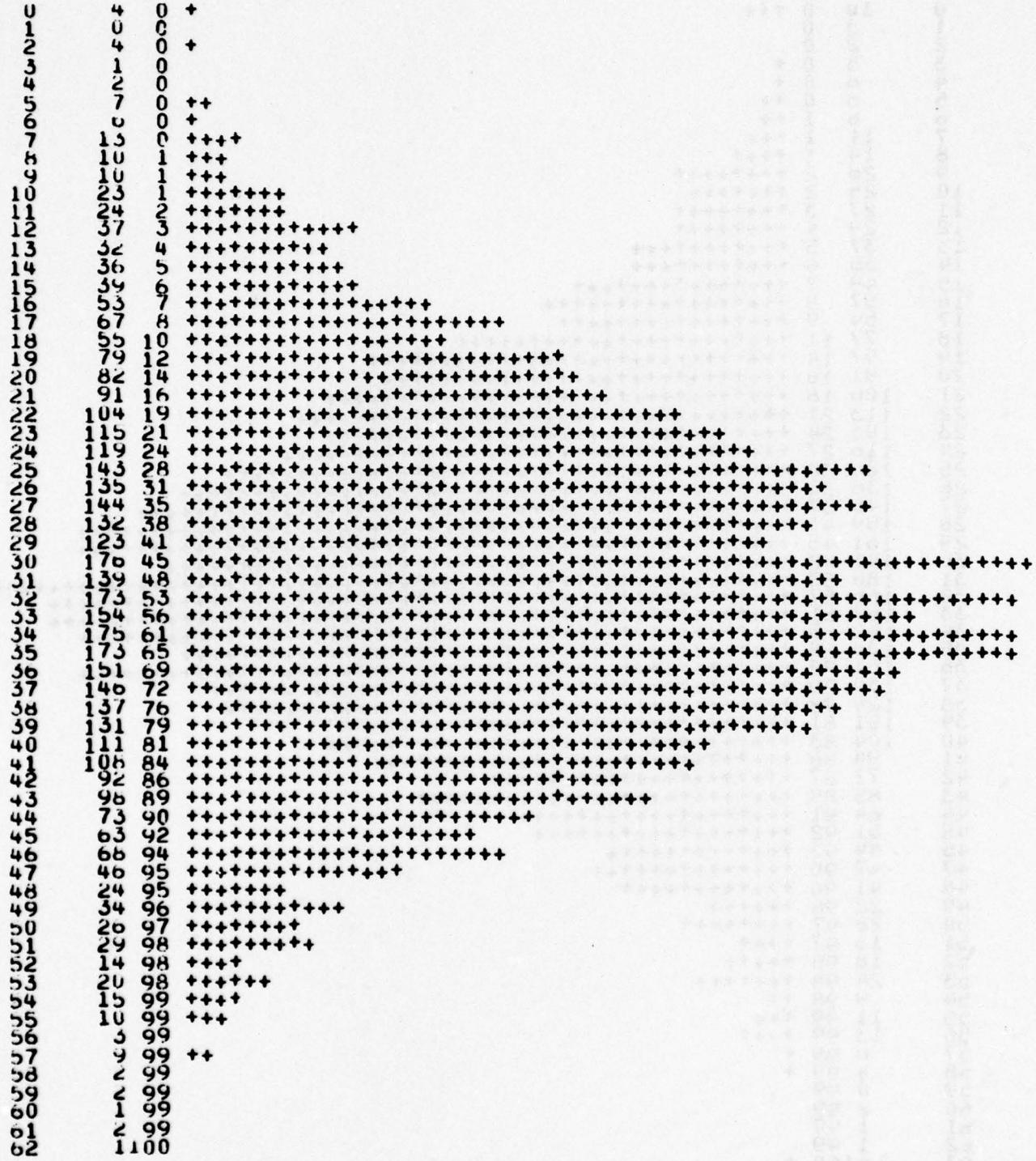

Figure 2b. $\rho = 0.75$

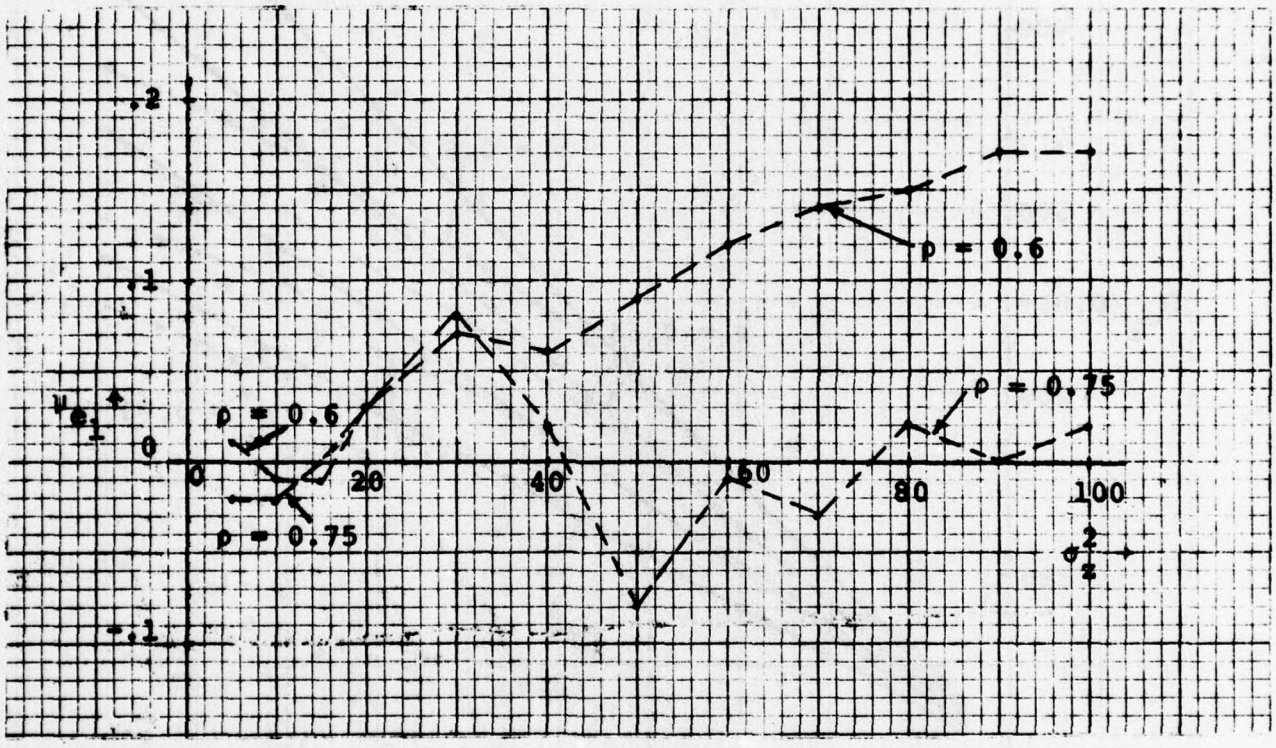

Figure 3. Statistical properties of the Laplacian responses as functions of σ_z^2,

dashed lines: estimated functions
solid lines: predicted functions

a. The mean values
(Predicted mean is zero for all σ_z^2)

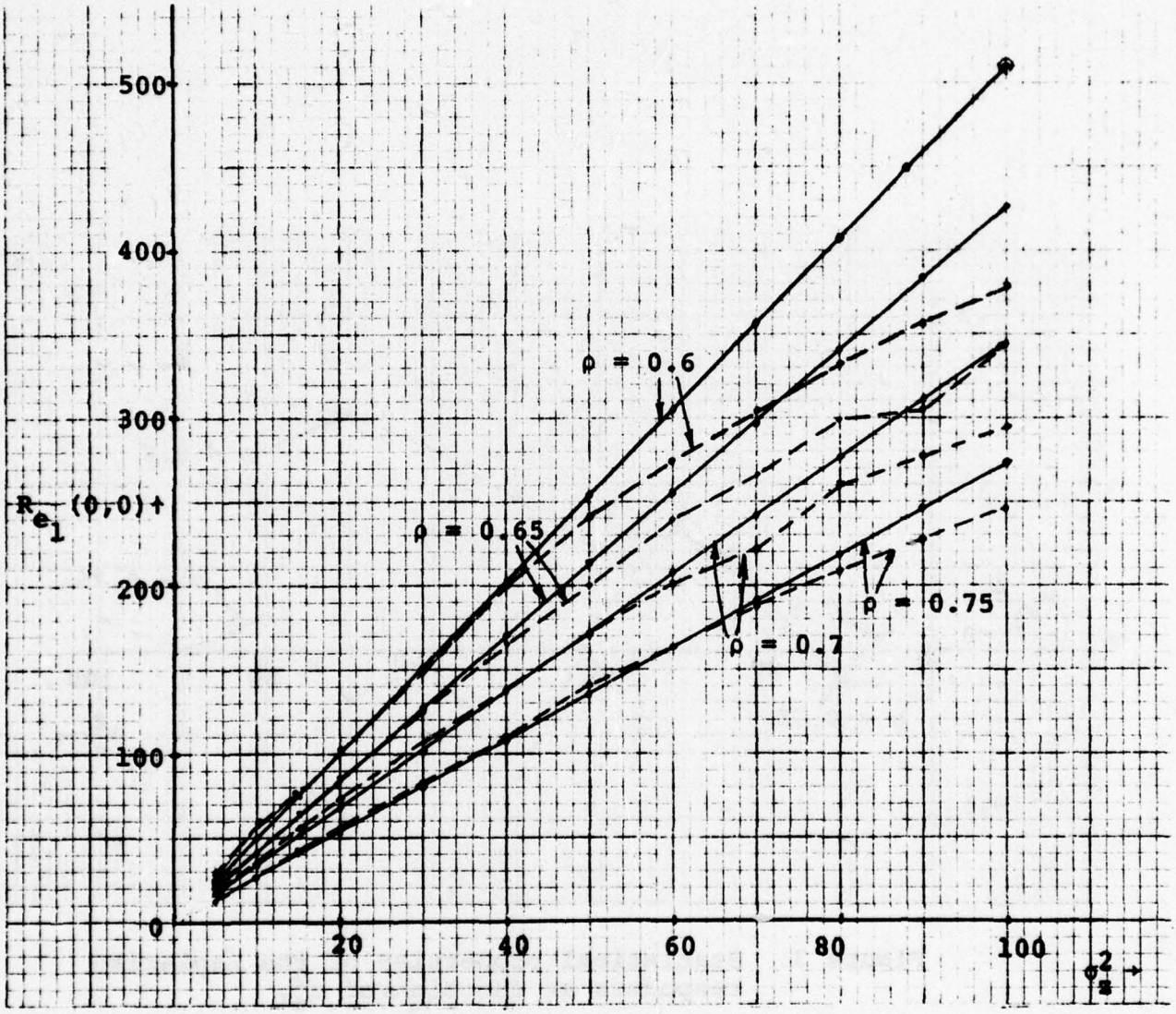

Figure 3b. The variances.

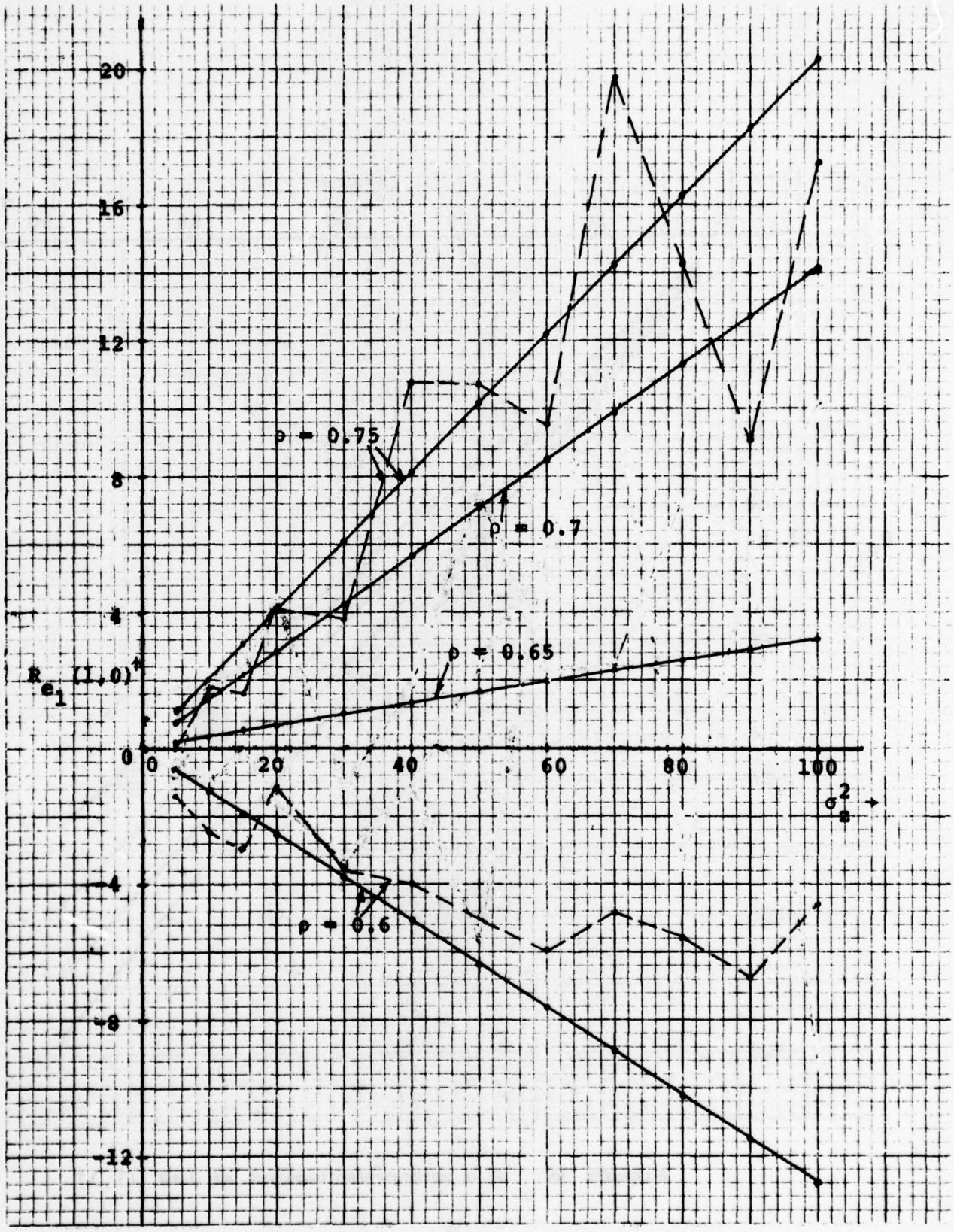

Figure 3c. The autocovariances at lag (1,0).

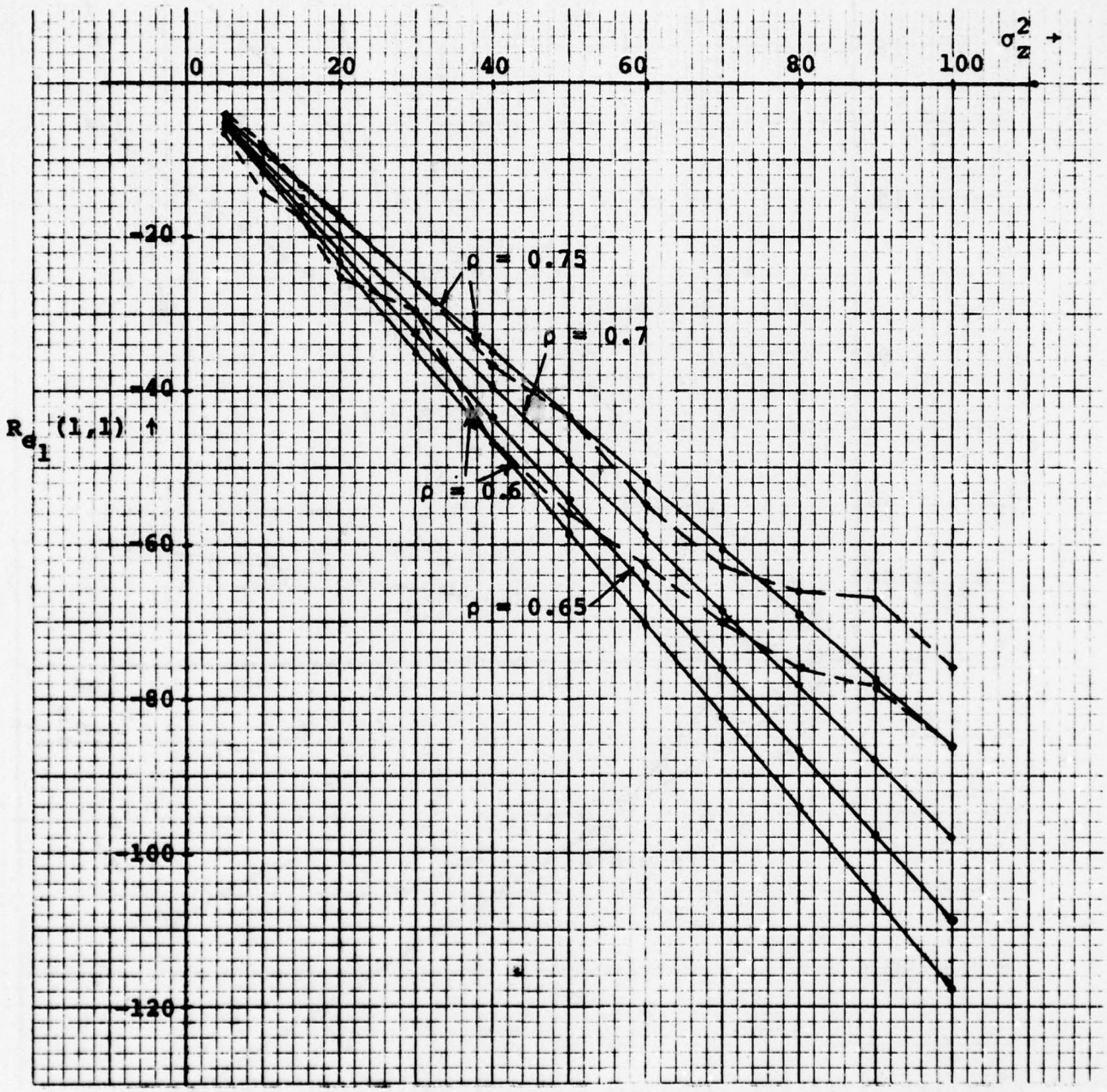

Figure 3d. The autocovariances at lag (1,1).

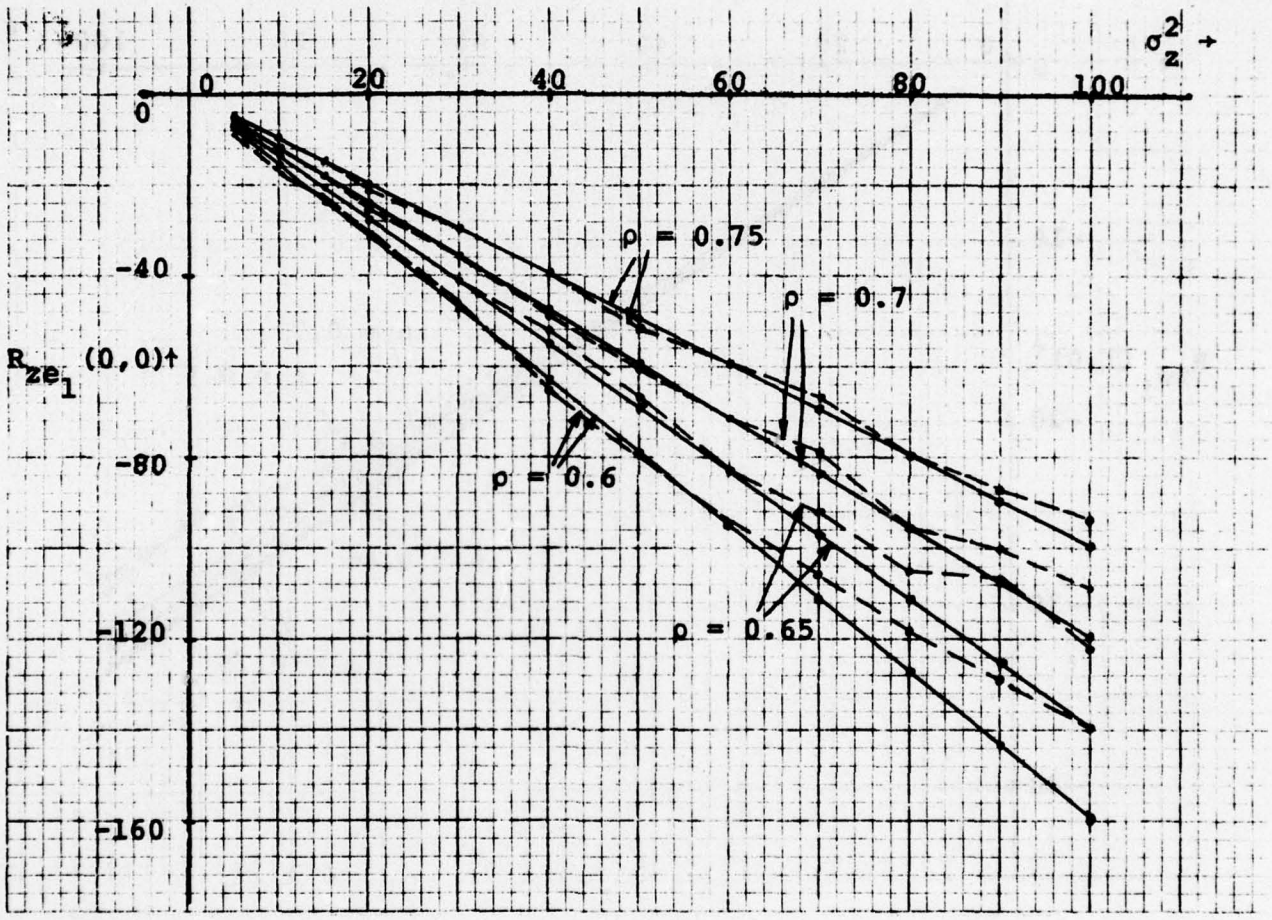

Figure 3e. The crosscovariances at lag (0,0).

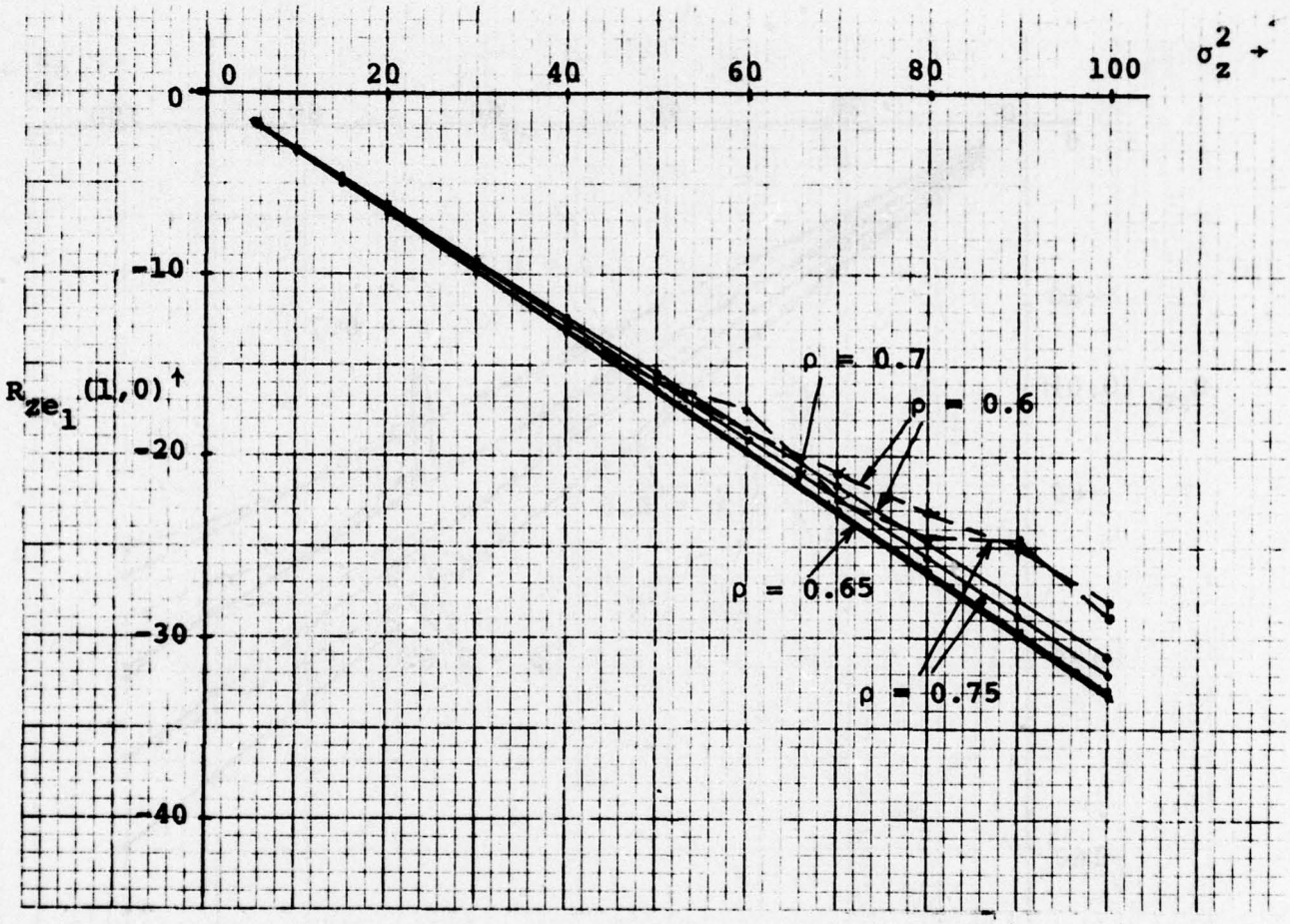

Figure 3f. The crosscovariances at lag (1,0).

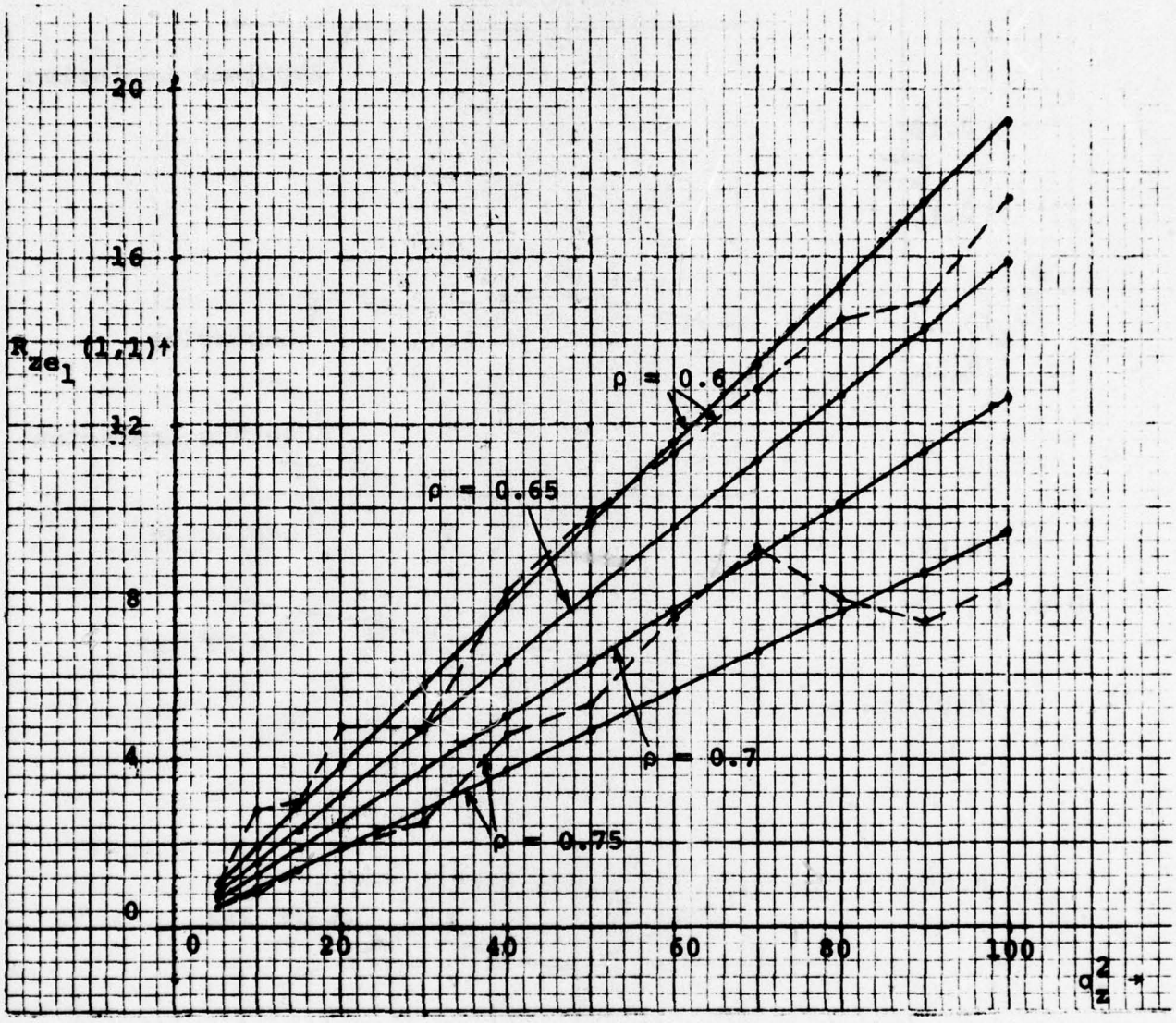

Figure 3g. The crosscovariances at lag (1,1).

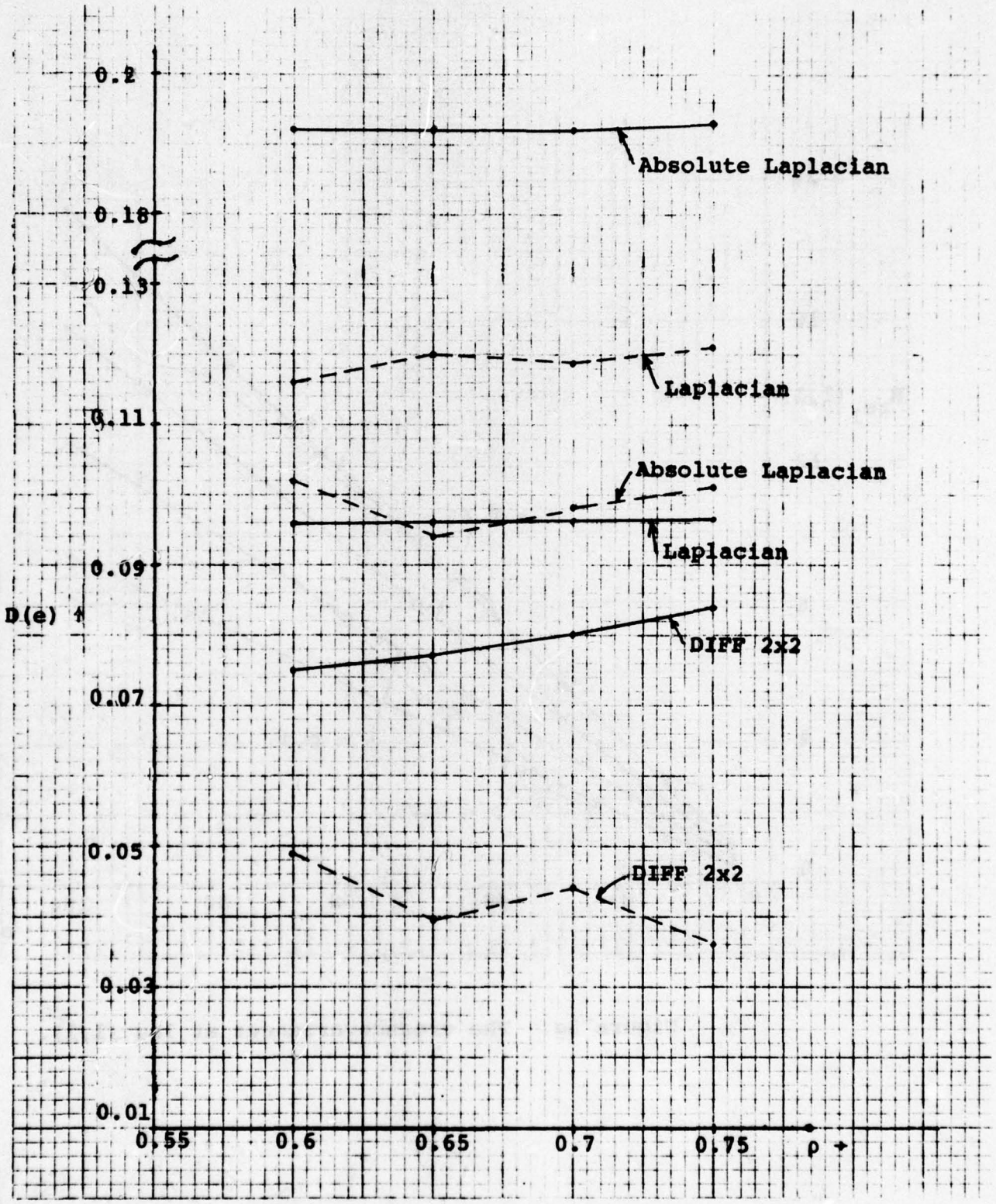

Figure 4. The densities of local maxima as functions of ρ,
dashed lines: estimated functions (for $\sigma_z^2 = 30$)
solid lines: predicted functions

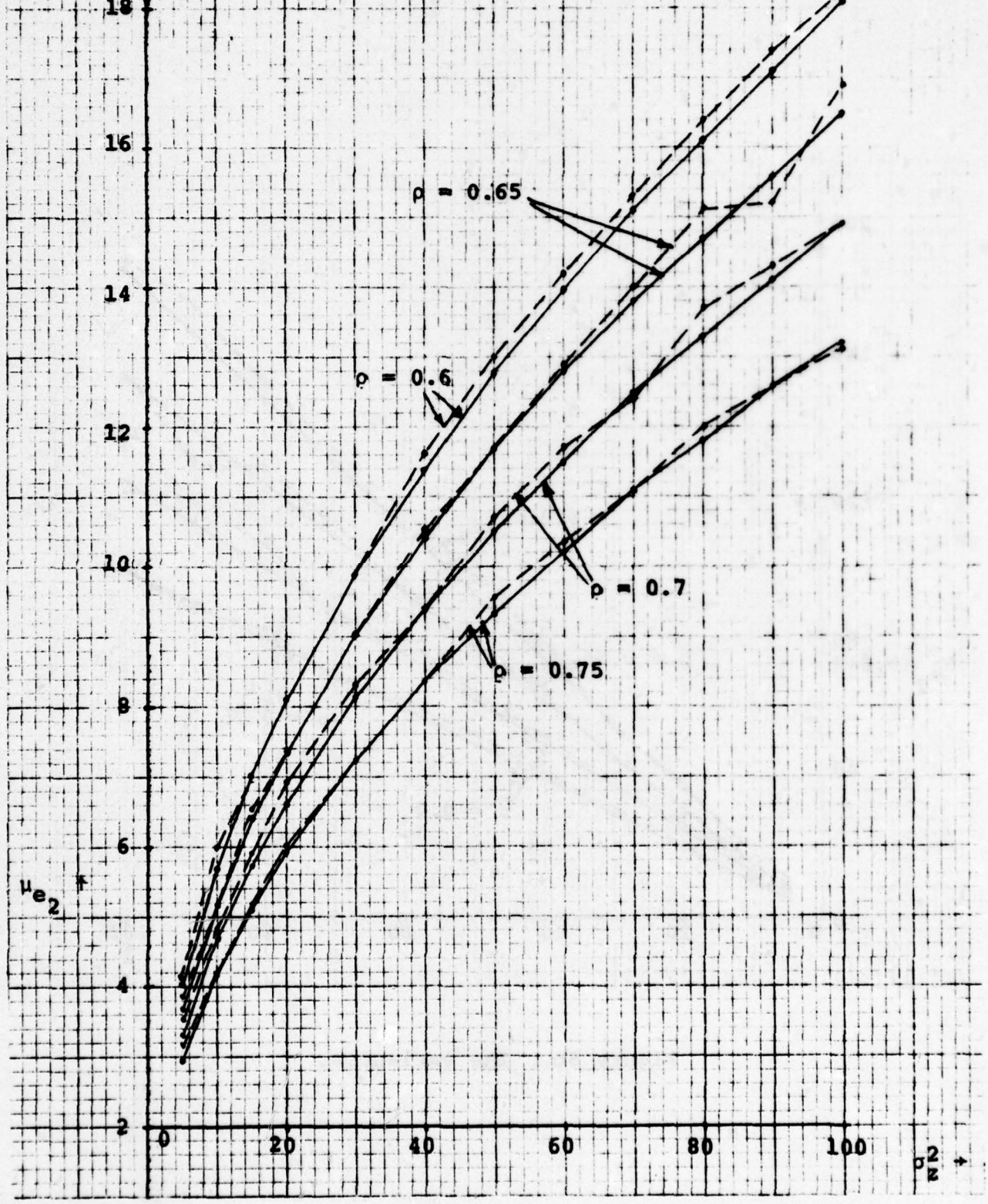

Figure 5. Statistical properties of the Absolute Laplacian responses as functions of σ_z^2, dashed lines: estimated functions solid lines: predicted functions.

a. The mean values.

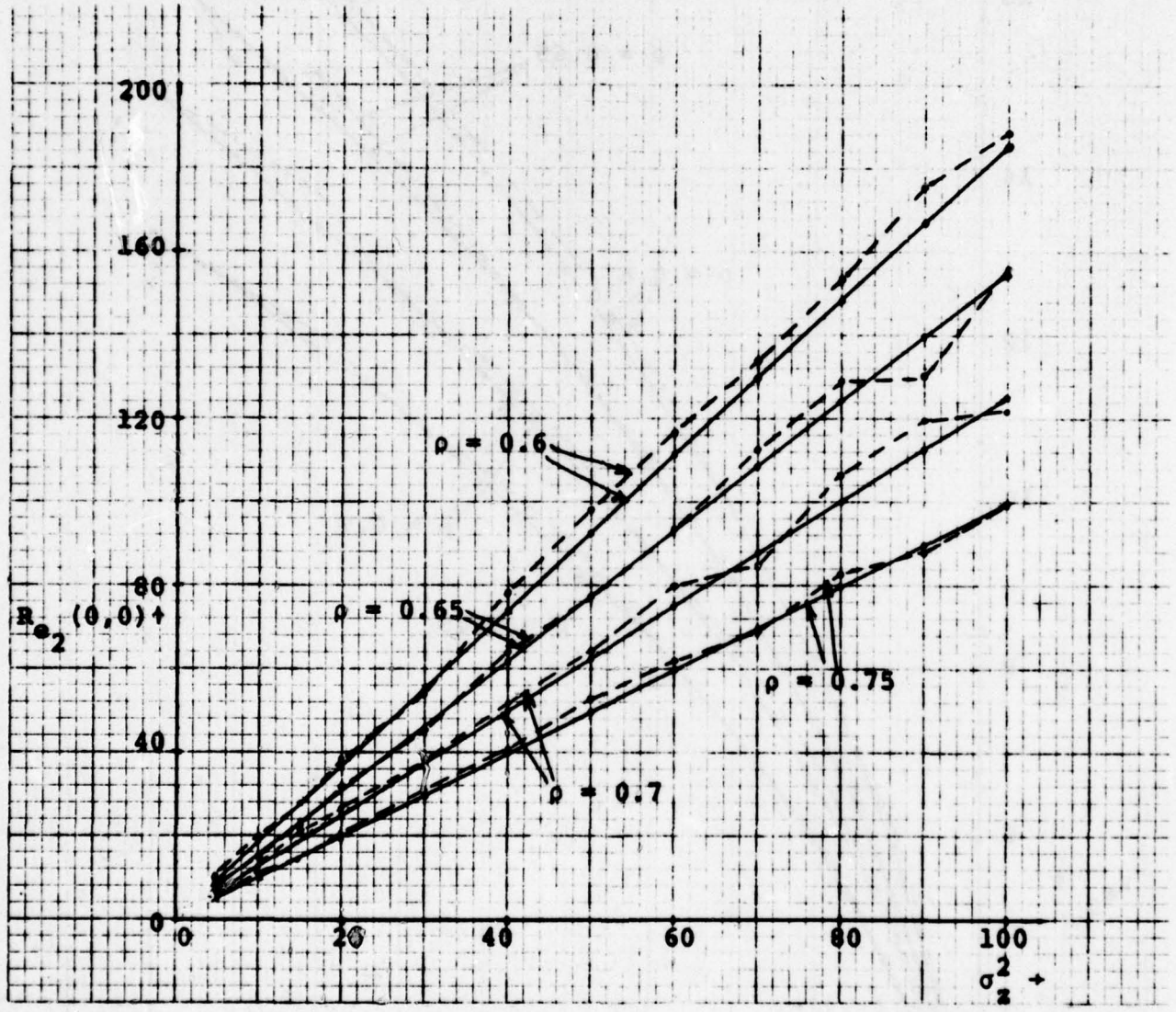

Figure 5b. The variances.

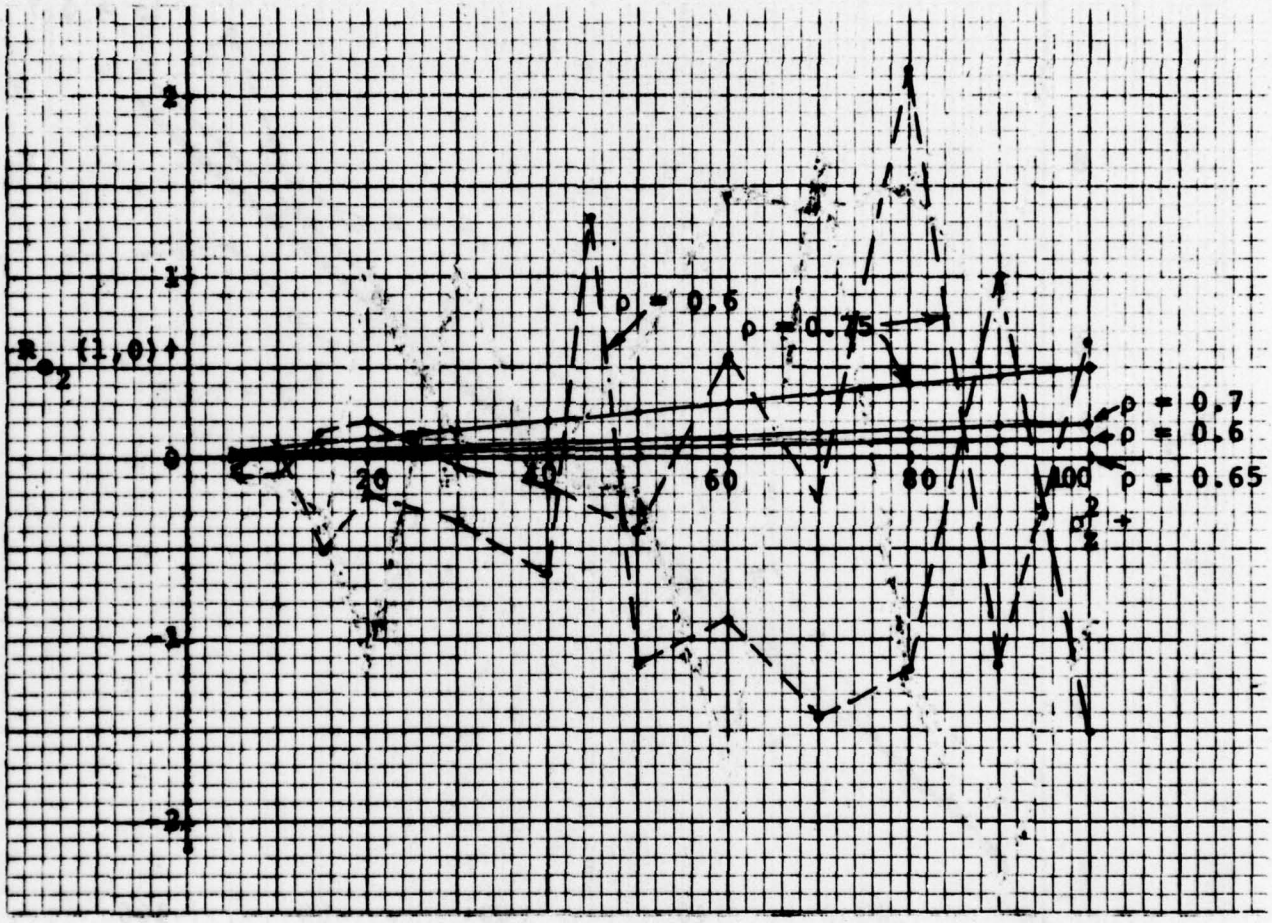

Figure 5c. The autocovariances at lag (1,0).

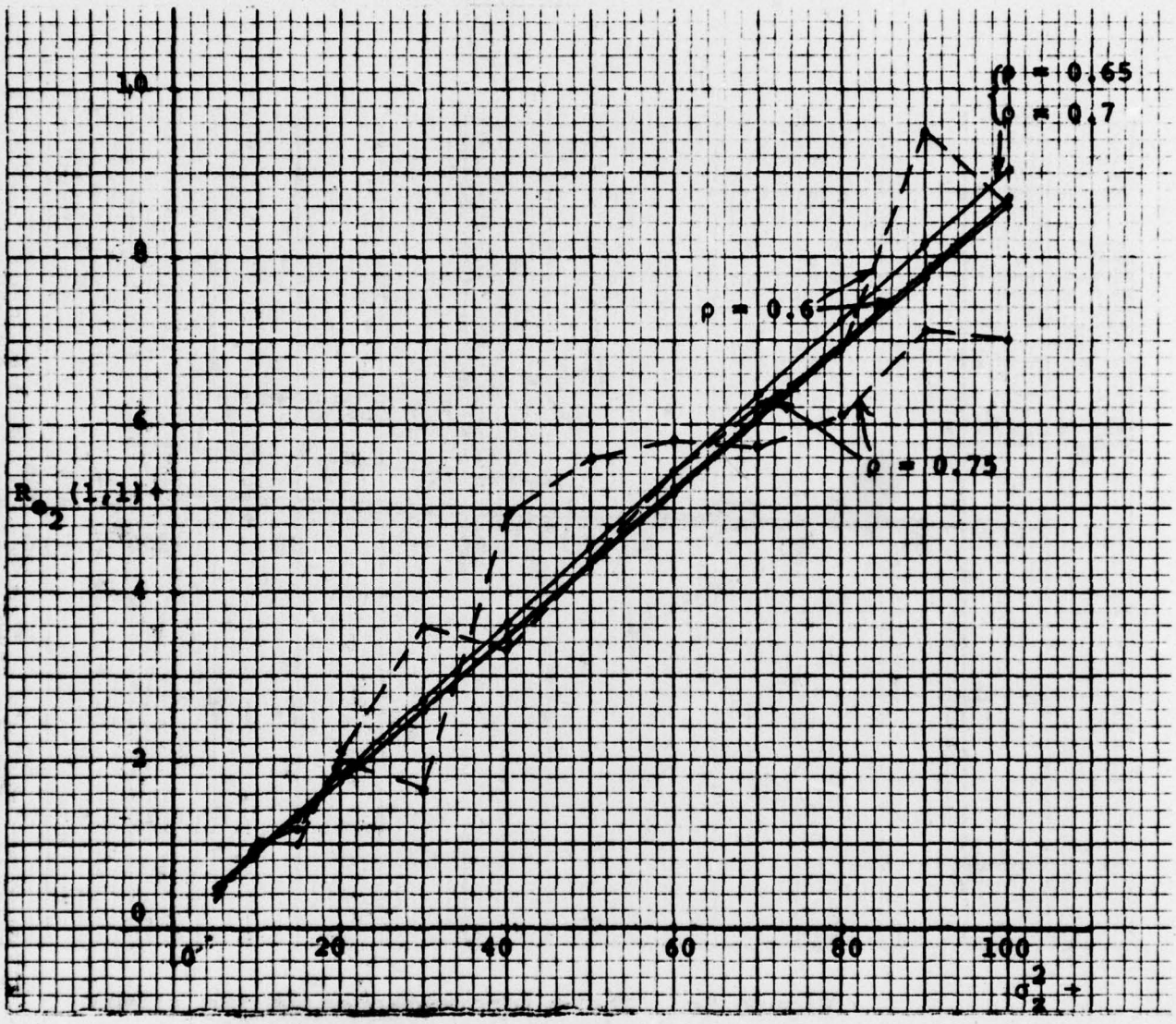

Figure 5d. The autocovariances at lag (1,1).

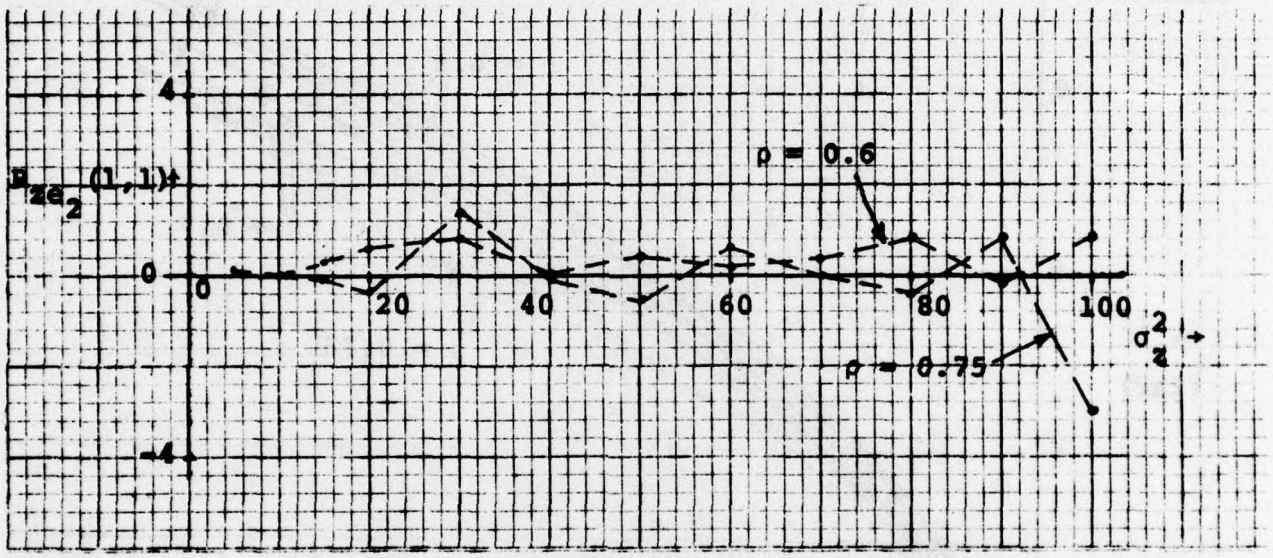

Figure 5e. Two sets of crossvariances (the predicted crosscovariances are zero for all ρ and σ_z^2).

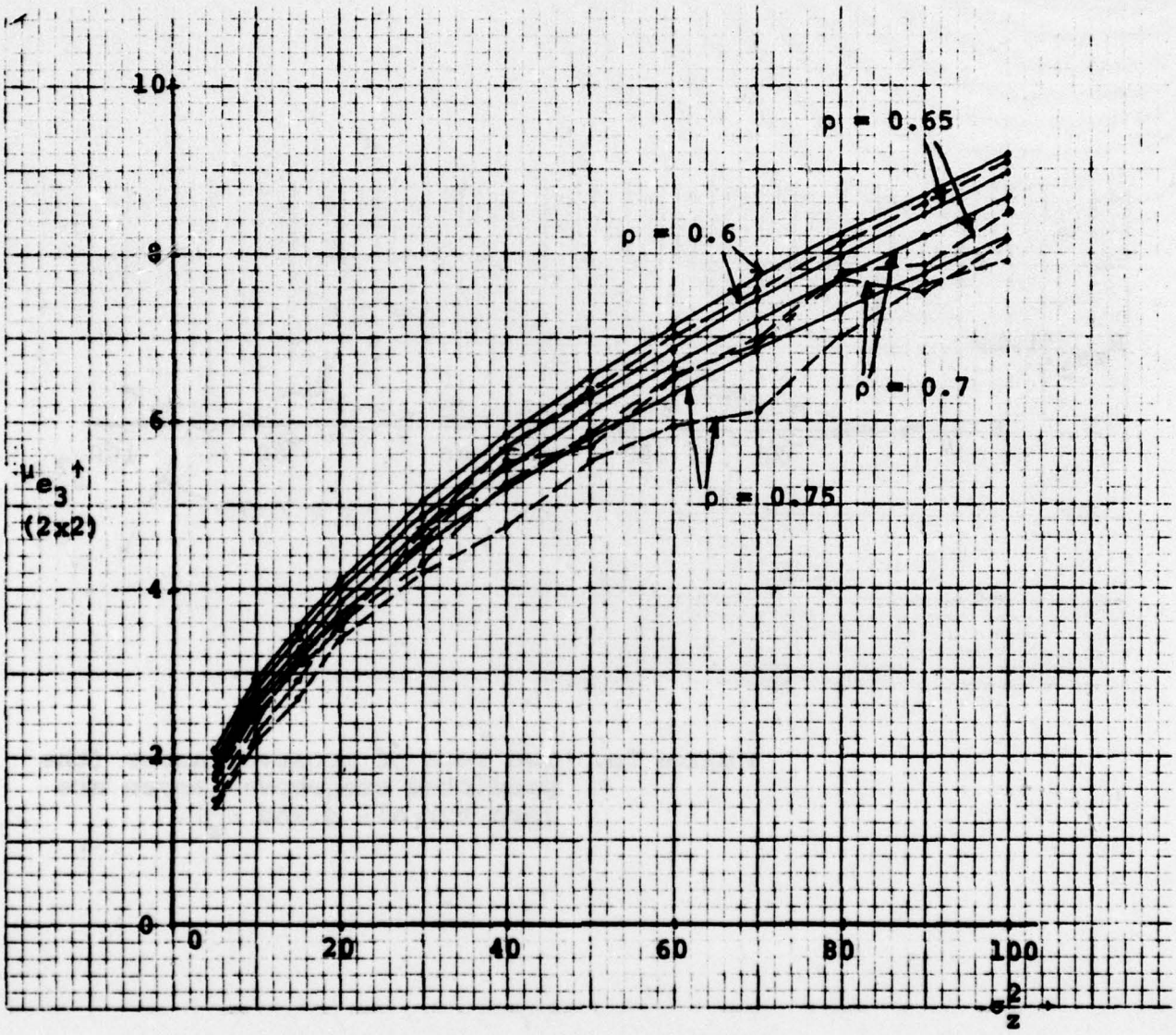

Figure 6. Statistical properties of the DIFF responses as functions of σ_z^2,

dashed lines: estimated functions
solid lines: predicted functions

a. The mean values of 2x2 DIFF.

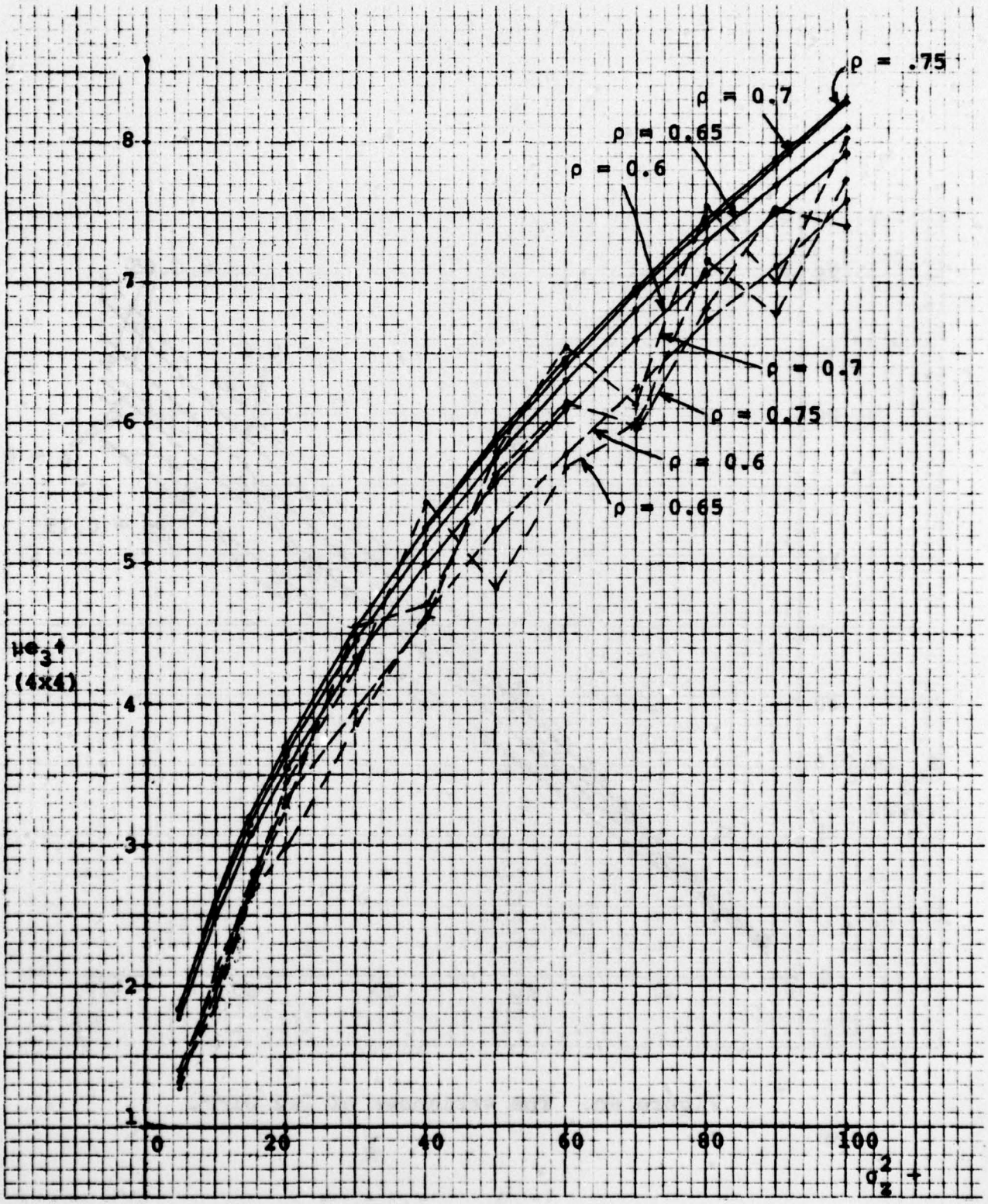

Figure 6b. The mean values of 4x4 DIFF.

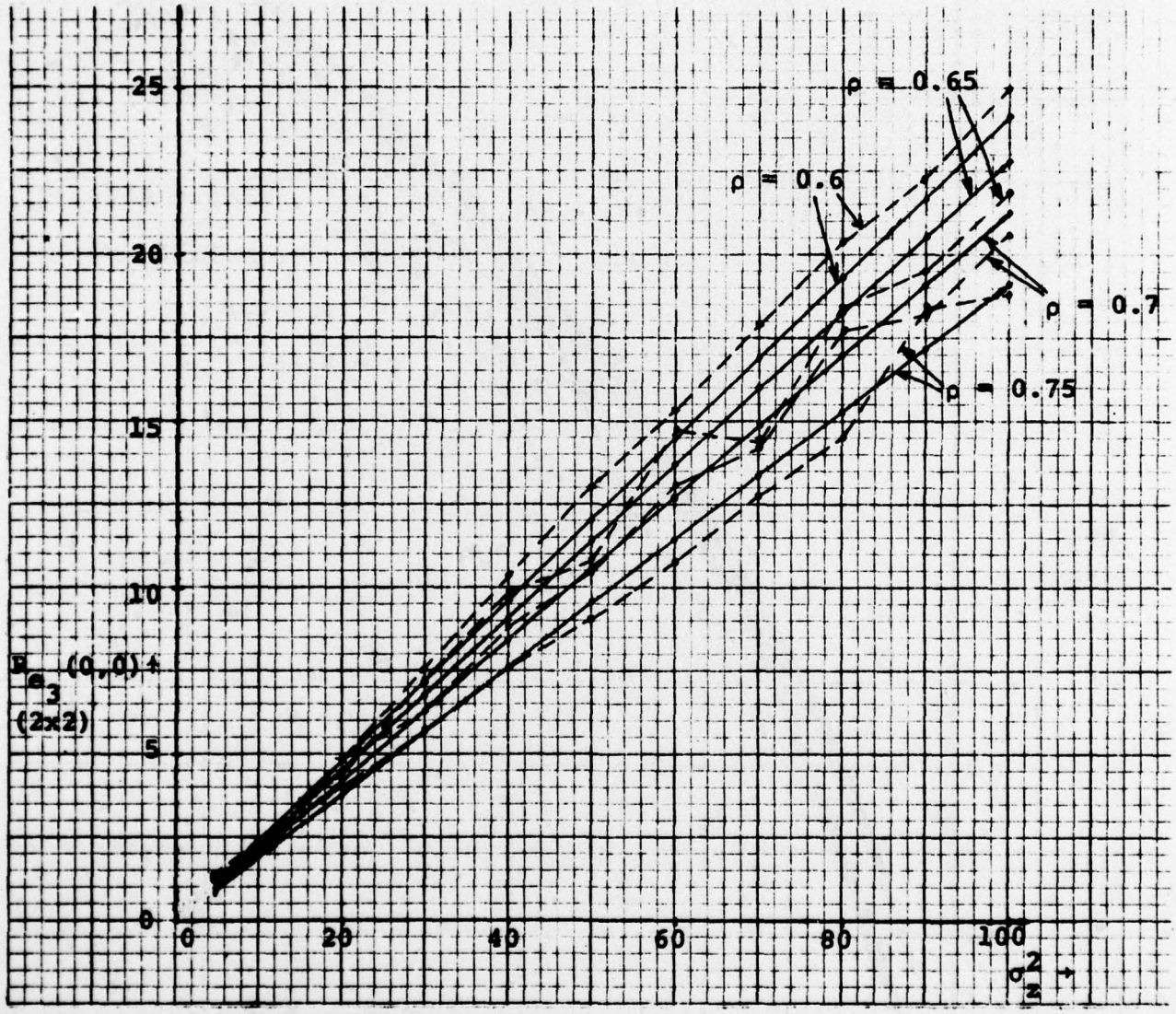

Figure 6c. The variances of 2x2 DIFF.

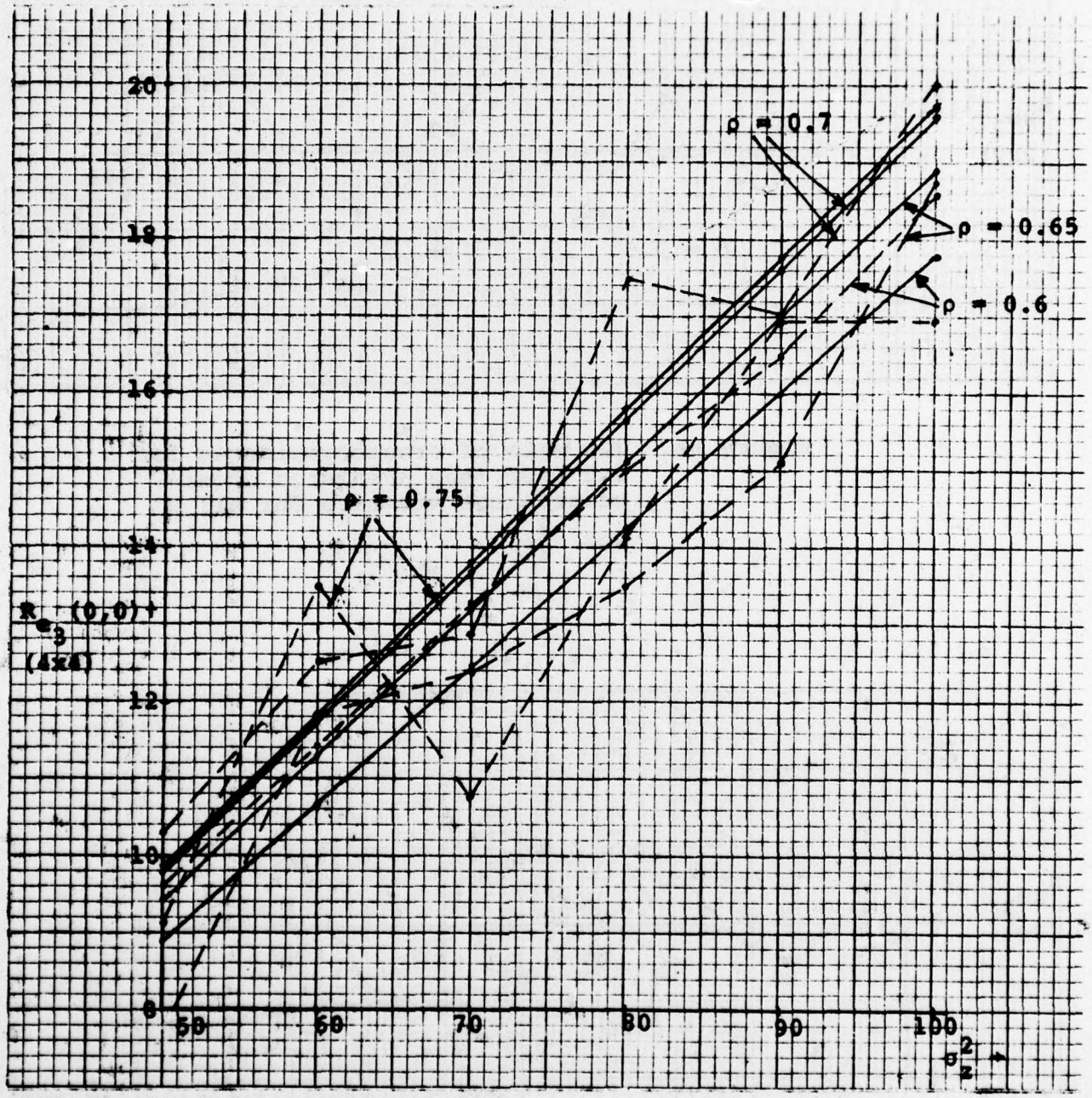

Figure 6d. The variances of 4x4 DIFF.

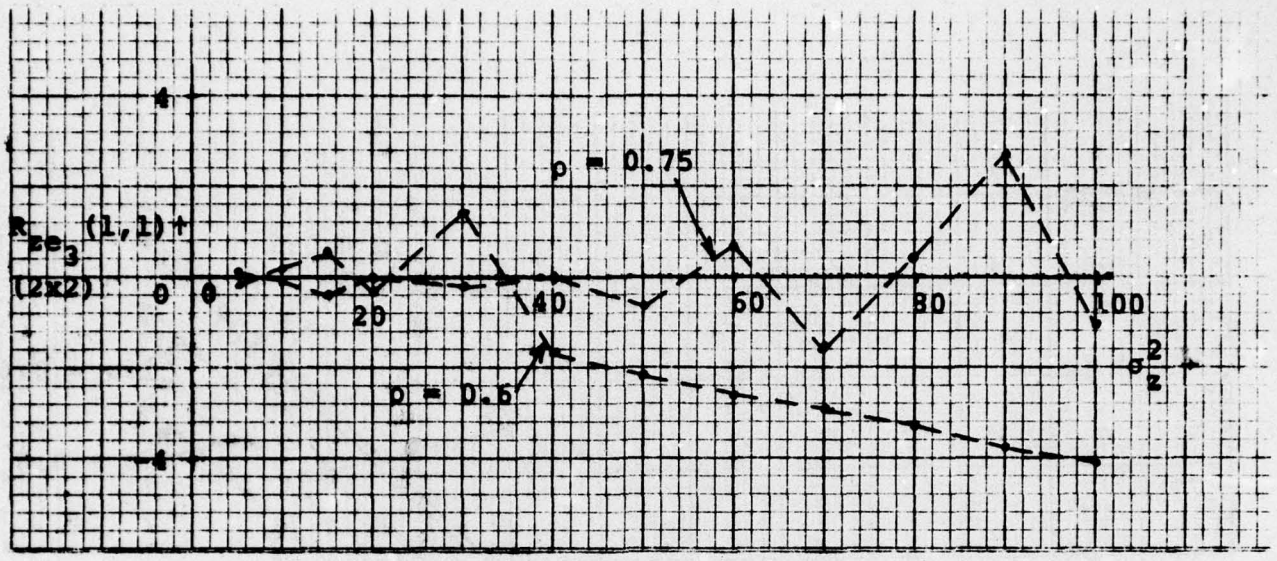

Figure 6e. Two sets of crosscovariances for 2x2 DIFF (the predicted cross-covariances are zero for all ρ and σ_z^2).

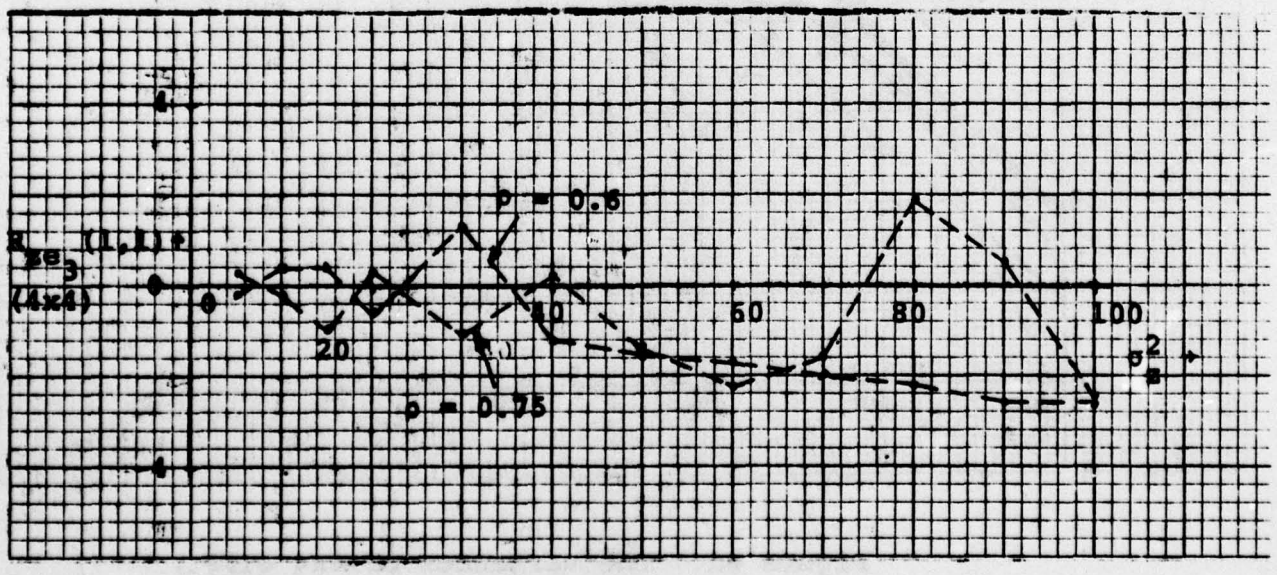

Figure 6f. Two sets of crosscovariances for 4x4 DIFF (the predicted cross-covariances are zero for all ρ and σ_z^2).

We chose to plot and compare the covariances rather than the covariance coefficients because estimation of the covariance coefficients requires normalizing by the corresponding estimated standard deviations which themselves can be sources of error.

The following observations can be made from the comparison of the predicted and the estimated graphs.

1) With a few exceptions the estimated functions seem to be in good agreement with the predicted ones. Some quantitative analysis of the effect of quantization on the estimates would be desirable.

2) The absolute Laplacian and the DIFF responses are uncorrelated with the corresponding input image gray levels. This justifies the assumption of uncorrelatedness made elsewhere [11] in the analysis of joint histograms.

3) For all $\rho < 0.9$ the predicted variance of the Laplacian response is larger than that of the input image. For input images with large variance the predicted variance can get so large that a considerable number of points will have edge values* outside the range of 0 to 63. Figure 7 shows the histograms of two such Laplacian responses. In these responses,

---

*The Laplacian responses have mean value zero. A constant value of 31 is added to the responses to translate the negative values to the positive domain.

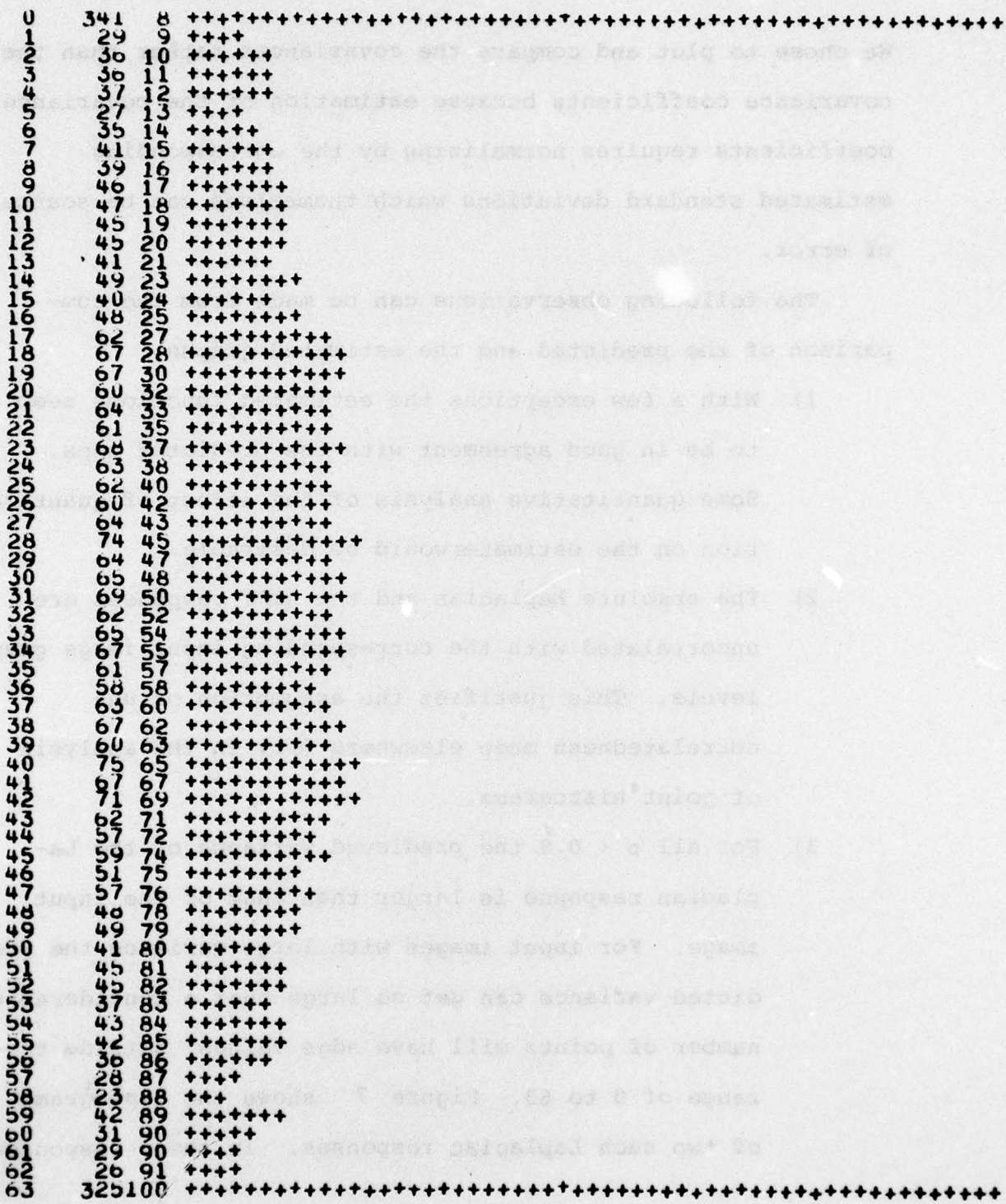

Figure 7. The histograms of the Laplacian responses to two of the test images with $m_2 = 100$.

a. $\rho = 0.6$

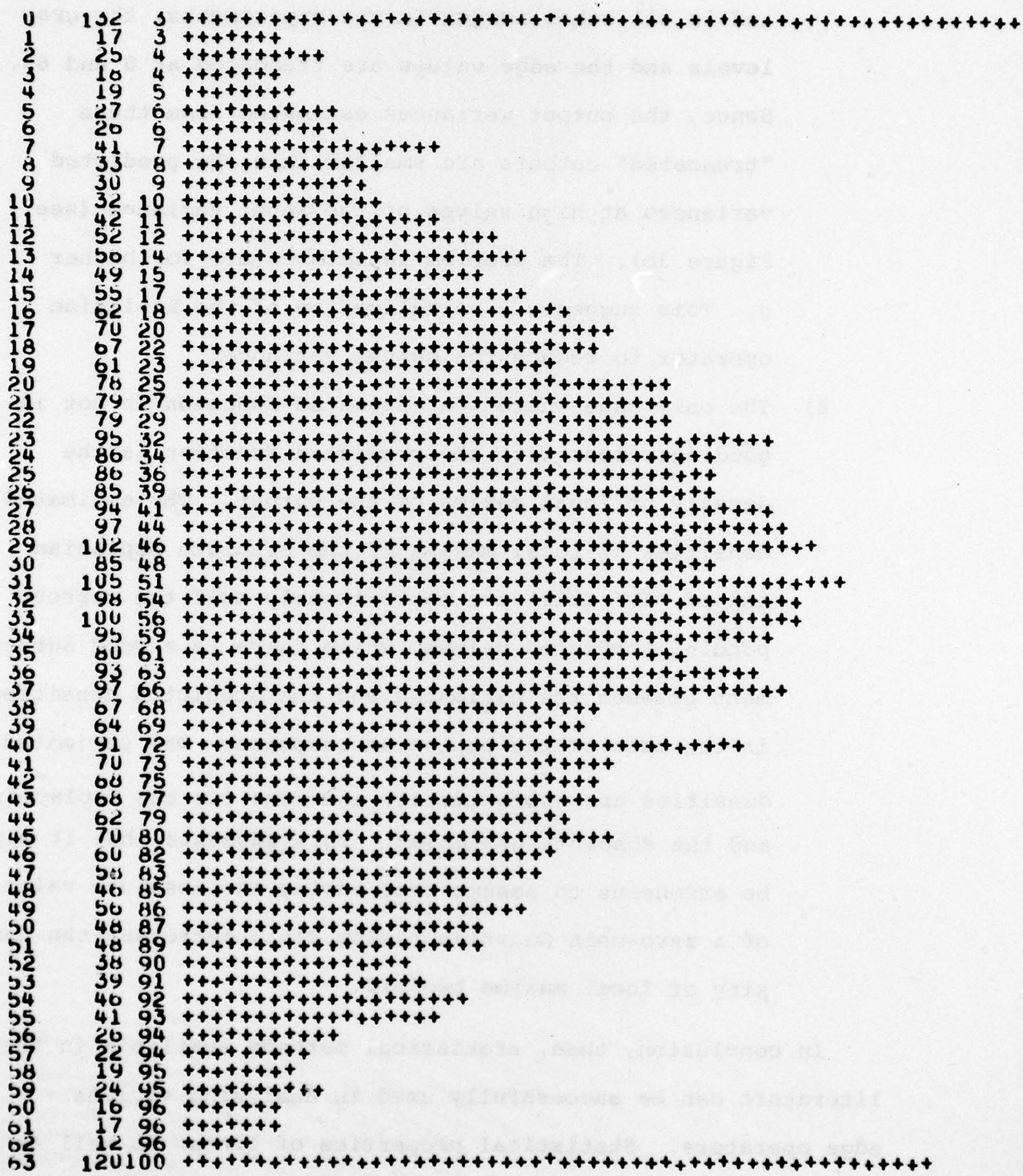

Figure 7b. $\rho = 0.75$.

and in all other images in the experiments, the gray levels and the edge values are truncated at 0 and 63. Hence, the output variances estimated from these "truncated" outputs are smaller than the predicted variances at high values of the input variance (see Figure 3b). The problem is less severe for higher ρ. This suggests a normalization of the Laplacian operator to reduce the output variance.

4) The only case where the estimated function is not in good agreement with the predicted function is the density of local maxima of the output. The estimated densities of local maxima of the absolute Laplacian and of DIFF (2x2) are approximately half the corresponding predicted values, while there is a good agreement between the estimated and the predicted densities in the case of the Laplacian responses. The estimated densities are approximately the same for the Laplacian and the absolute Laplacian. This suggests that it may be erroneous to assume that taking the absolute value of a zero-mean Gaussian random field increases the density of local maxima twofold.

In conclusion, then, statistical methods available in the literature can be successfully used in analyzing various edge operators. Statistical properties of linear as well as nonlinear edge operators can be predicted using the power spectrum of the input image. Experiments with synthetic data

having a given image power spectrum indicate reasonable accuracy of prediction. Successful application to real images will depend on the accuracy of the power spectrum model used. More insight into the choice of power spectrum for real images should be obtained by further experimentation.

References

1. A. Rosenfeld and A. C. Kak, Digital Picture Processing, Academic Press, New York, 1976.

2. M. S. Longuet-Higgins, "The statistical analysis of a random moving surface", Phil. Trans. Roy. Soc. London, vol. A249, pp. 321-387, February 1957.

3. P. Whittle, "On stationary processes in the plane", Biometrika, vol. 41, pp. 434-449, 1954.

4. W. Freiberger and U. Grenander, Surface Patterns in Theoretical Geography, Reports on Pattern Analysis, no. 41, Division of Applied Mathematics, Brown University, Providence, RI, September 1976.

5. B. R. Hunt and T. M. Cannon, "Nonstationary assumptions for Gaussian models of images", Correspondence, IEEE Trans. on Syst., Man, and Cyb., vol. SMC-6, no. 12, pp. 876-882, December 1976.

6. M. S. Longuet-Higgins, "Statistical properties of an isotropic random surface", Phil. Trans. Roy. Soc. London, vol. A250, pp. 157-171, October 1957.

7. R. Price, "A useful theorem for nonlinear devices having Gaussian inputs", IRE Trans. on Inf. Th., vol. IT-4, no. 2, pp. 69-72, June 1958.

8. R. Price, "Comments on: A useful theorem for nonlinear devices having Gaussian inputs", Correspondence, IEEE Trans. on Inf. Th., vol. IT-10, no. 2, pp. 171, April 1964.

9. K. C. Hayes, Jr. and A. Rosenfeld, Efficienct Edge Detectors and Applications, Tech. Rep. no. 207, Computer Science Center, Univ. of Maryland, College Park, MD, November 1972.

10. E. L. McMahon, "An extension of Price's theorem", Correspondence, IEEE Trans. on Inf. Th., vol. IT-10, no. 2, pp. 168, April 1964.

11. D. P. Panda, "Segmentation of FLIR images by pixel classification", Proc. DARPA Image Understanding Workshop, pp. 65-70, April 1977.

UNCLASSIFIED

SECURITY CLASSIFICATION OF THIS PAGE (When Data Entered)

REPORT DOCUMENTATION PAGE		READ INSTRUCTIONS BEFORE COMPLETING FORM
1. REPORT NUMBER	2. GOVT ACCESSION NO.	3. RECIPIENT'S CATALOG NUMBER
4. TITLE (and Subtitle) STATISTICAL ANALYSIS OF SOME EDGE OPERATORS		5. TYPE OF REPORT & PERIOD COVERED Technical
		6. PERFORMING ORG. REPORT NUMBER TR-558
7. AUTHOR(s) Durga P. Panda		8. CONTRACT OR GRANT NUMBER(s) DAAG53-76C-0138
9. PERFORMING ORGANIZATION NAME AND ADDRESS Computer Science Ctr. Univ. of Maryland College Pk., MD 20742		10. PROGRAM ELEMENT, PROJECT, TASK AREA & WORK UNIT NUMBERS
11. CONTROLLING OFFICE NAME AND ADDRESS U. S. Army Night Vision Lab. Ft. Belvoir, VA 22060		12. REPORT DATE July 1977
		13. NUMBER OF PAGES
14. MONITORING AGENCY NAME & ADDRESS(if different from Controlling Office)		15. SECURITY CLASS. (of this report) Unclassified
		15a. DECLASSIFICATION/DOWNGRADING SCHEDULE

16. DISTRIBUTION STATEMENT (of this Report)

Approved for public release; distribution unlimited.

17. DISTRIBUTION STATEMENT (of the abstract entered in Block 20, if different from Report)

18. SUPPLEMENTARY NOTES

19. KEY WORDS (Continue on reverse side if necessary and identify by block number)

Statistical analysis
Edge operators
Image modeling

20. ABSTRACT (Continue on reverse side if necessary and identify by block number) A statistical analysis of the responses of some linear and nonlinear edge operators is presented. The input image is treated as a stationary random field from a context independent ensemble. Several stochastic properties of the output images are predicted. Some experimental results are given.

DD FORM 1 JAN 73 1473 EDITION OF 1 NOV 65 IS OBSOLETE

UNCLASSIFIED

SECURITY CLASSIFICATION OF THIS PAGE (When Data Entered)